The use of a 3D Sonic Anemometer for the Study of Airflow Patterns in a Hospital Patient Room

A Thesis

Presented in Partial Fulfilment of the Requirements for the

Degree of Master of Science

with a

Major in Integrated Architecture and Design

in the

College of Graduate Studies

University of Idaho

by

Chinmayee Milind Patil

Major Professor: Elizabeth Cooper, M.S.

Committee Members: Ralph Budwig, Ph.D.; Bruce Haglund, M. Arch.

Department Administrator: Randall Teal, MIARC.

December 2017

Authorization to Submit Thesis

This thesis of Chinmayee Milind Patil, submitted for the degree of Master of Science with a major in Integrated Architecture and Design and titled "The use of a 3D Sonic Anemometer for the Study of Airflow Patterns in a Hospital Patient Room," has been reviewed in final form. Permission, as indicated by the signatures and dates given below, is now granted to submit final copies to the College of Graduate Studies for approval.

Major Professor: _____Date_____
Elizabeth Cooper, M.S.

Committee Members: _____Date_____
Ralph Budwig, Ph.D.

_____Date_____
Bruce Haglund, M. Arch.

Department Administrator: _____Date_____
Randall Teal, MIARC.

Abstract

Efficient ventilation can contribute to reducing the cooling and heating energy consumption of buildings, increasing the comfort level of the residents, and minimizing the risk of airborne infection in hospital rooms [72]. The dominant factor that affects the transmission and control of contaminants is the path between the contaminant source and exhaust. This understanding can be achieved with validated computational fluid dynamics (CFD) computer simulations, or with experimental techniques, such as measurements with smoke, neutrally buoyant markers, tracer gasses or tracer aerosol particles. As a supplementary technique to quantify airflows, the use of a state-of-the-art, three-dimensional sonic anemometer was explored. In this paper, we investigate ventilation in a patient room considering forced (mechanical) ventilation. This instrument allows for the precise measurement of the air velocity vector components in the range of a few centimeters per second, which is common in many indoor environments. Measurements of air velocities and directions at selected locations were made for the purpose of studying the airflow patterns in a mechanically ventilated patient room.

Acknowledgements

This paper would not have been possible without the work and dedication of several individuals who have been guiding me through the research process. I wish to express my sincerest gratitude to my major professor Elizabeth Cooper for her continuous support, motivation, and expertise during this research. She not only acted as thesis advisor but also as a mentor who has spent many long hours helping in my development as a student and as a person. Besides my advisor, I would like to thank you my thesis committee, Prof. Ralph Budwig for his guidance throughout my tenure at U of I. He helped me to develop my background in Experimental Fluid Mechanics. I'm forever grateful for his guidance with the courses as well as with my research and to Prof. Bruce Haglund for his insightful comments and encouragement.

My sincere thanks to Jesse Barnum and Russell Harbaugh for giving me an access to the test facility. I would like to extend my thanks to Bob Basham for helping me with anemometer setup and my friends and fellow graduate students at the Integrated Design lab, especially Damon Woods who was always willing to help, give his best suggestions. My research would not have been possible without their help.

Finally, I must express my very profound gratitude to my parents for their love and unfailing support through my life. I'm immensely grateful to my husband, Chinmay who has been a constant source of support and encouragement during the challenges of graduate school and life. My heartfelt regards go to my brother, father in law and mother in law for their love and support. I would also like to thank you my uncle for encouraging me to pursue this degree and for his invaluable guidance.

I thank the Almighty for showering his blessings and giving me the strength and patience to pursue this passion with sheer excitement and determination.

Table of Contents

List of Tables

List of Figures

CHAPTER 1

Introduction

Airborne transmission of disease occurs by dissemination of either airborne droplet nuclei or small particles in the respirable size range containing infectious agents that remain infective over time and distance (e.g., spores of Aspergillus spp, Mycobacterium tuberculosis). Microorganisms carried in this manner may be dispersed over long distances by air currents and may be inhaled by susceptible individuals who have not had face-to-face contact with (or been in the same room with) the infectious individual [1-4].

The design of proper, general ventilation systems can play an important role in preventing the spread of infections. Patients with infectious diseases that spread easily through the air (e.g. chickenpox, measles, and tuberculosis) should be placed in airborne precaution rooms. However, there is often a delay between admission of these patients to the health-care facility and the diagnosis of their infectious disease. Disease transmission to other patients or staff can occur while these patients are waiting in common areas (e.g. waiting room, emergency departments). Paying more attention to ventilation requirements in these common, non-isolation spaces could lead to significant infection-control benefits [50].

In addition to occupant comfort, heating, ventilation, and air conditioning (HVAC) systems should provide indoor air quality (IAQ) continuously. As a result, hospital HVAC is generally not load-driven, but is predicated on providing adequate ventilation air to maintain a wide range of directional airflow relationships (from cleaner to less clean spaces) and air change rates to contain, dilute and remove hazards such a volatile medical gases, particulates, and airborne diseases [12]. The Wells-Riley equation supports the premise that increasing the volume of "clean" air dilutes the room air and thus exposes people in the room to fewer potentially infectious particles. Air change per hour (ACH) is the only variable in the Wells-Riley equation that can be quantified by direct measurement.

$$N_c = S(1 - e^{(-Iqpt/Q)}) \tag{1.1}$$

Here I is the number of infective, S is the susceptible people in a space, Q is the room ventilation rate in m^3/s, N_c is the quantity of infectious material in the air to predict the number of new cases infected over a period of time t (s) and p (m^3/s) is the pulmonary ventilation rate of susceptible individuals, while q represents a unit of infection termed as 'quantum', introduced by Wells (1955) [70], to express the response of susceptible individuals to inhaling infectious droplet nuclei [71].

Our knowledge of the effect of the many other variables (e.g., infectious dose, relative humidity, temperature, host susceptibility, chain of transmission) on disease transmission is limited [56]. Most studies on the transmission of infectious airborne disease have focused on patient room air changes per hour (ACH) and how ACH provides pathogen dilution and removal. The logical but mostly unproven premise is that greater air change rates reduce the concentration of infectious particles and thus, the probability of airborne disease transmission. Recently, a growing body of research suggests pathways between the pathogenic source (patient) and control (exhaust) may be the dominant environmental factor [11]. While increases in airborne disease transmission have been associated with ventilation rates below 2 ACH, comparatively less data is available to quantify the benefits of higher air change rates in clinical spaces (general patient rooms and isolation rooms) [11]. Although one-third of healthcare-acquired infections may involve airborne transmission at some point [13], only a few diseases like Measles, Severe Acute Respiratory Syndrome (SARS), Varicella (chickenpox), and Mycobacterium tuberculosis currently require infectious airborne isolation. To reduce both the concentration and time patients and healthcare workers are exposed to pathogenic microorganisms, ASHRAE Standard 170 and several other guidelines recommend 6-12 ACH for infectious isolation rooms and 4 ACH for patient rooms [14-17]. Although higher air change rates can better dilute contaminant concentrations within a patient room, air changes alone have not proven to reduce the risk of the airborne cross-infection [18-22]. A study of 1,289 healthcare workers in 17 Canadian hospitals found the risk of tuberculosis transmission was 3 to 4 times higher in patients rooms with <2.0 ACH

when compared to patient >2.0 ACH [44]. The healthcare workers who work at least 2 days per week underwent skin tests for tuberculosis and completed a survey. The researchers reviewed the records of all patients with tuberculosis who were hospitalized at each hospital during the previous 3 years. The researchers also did tests of ventilation that measured air flow at various locations in the hospital. They then looked for associations between hospital ventilation and positive test results for tuberculosis in hospital workers. Positive test results for tuberculosis were associated with poor ventilation in general patient rooms. However, negative test results for tuberculosis were obtained with the ventilation in isolation rooms. This is probably because hospital workers usually wear masks when they enter isolation rooms [57]. Mousavi [11] conducted a series of tests in an actual hospital to observe the containment and removal of respirable aerosols ($0.5 - 10$ μm) with respect to ventilation rate and directional airflow in a general patient room, and, an airborne infectious isolation room. Higher ventilation rates were not found to be proportionately effective in reducing aerosol concentrations. Specifically, increasing mechanical ventilation from 2.5 to 5.5 ACH reduced aerosol concentrations only 30% on average. However, particle concentrations were more than 40% higher in pathways between the source and exhaust as was the suspension and migration of larger particles ($3 - 10$ μm) throughout the patient room(s) [11]. Empirical and numerical test results suggest that turbulence created by higher air change rates could reduce the benefits of bioaerosol removal by suspending infectious particles within breathing zone (1.2-1.8 m) [11]. Case studies on aircraft and other vehicles, schools, hospitals and other buildings with sick building syndrome, as well as some animal studies, suggest that regardless of actual ACH, ventilation rate is just one of many factors that affect the transmission of infectious disease [56]. Most studies do not account for the amount of time an infected individual spent in the space [22]. Crane (1994) notes an observation by Chatigny and West (1976) that increasing ventilation rates from 6 to 30 ACH has a minimal effect on the aerosol concentration of microorganisms in the first few minutes after release [56].

The guidelines for ventilation of ward spaces (i.e. ASHRAE 170-2008) contain air change

rates six air changes per hour (6 ACH) for general wards; which was selected by computational fluid dynamics modeling analysis [51]. However, after reviewing evidence from literature [27] Beggs concluded that studies on ward ventilation showed that the average residence time for particles at 6 ACH flow rate is 10 minutes as opposed to 30 minutes when 2 ACH is used, as was previously the standard. These findings show that the advantages of increasing ACH in terms of improving environments in the rooms may have limits and warrants further investigation [56]. Apart from providing minimum relative ventilation rates, ASHRAE guidelines provide no insight into how desirable airflow patterns and direction can be achieved in hospital spaces. A World Health Organization (2009) report on the use of natural ventilation notes that where droplet nuclei are an important mode of disease transmission, average quanta production rates in subjects are usually <1 quanta/minute. With a quanta production rate of 10 quanta/minute, the estimated risk of infection with 15 minutes of exposure in a room with 12 ACH is 4 percent, and with 24 ACH it is 2 percent. This illustrates the importance of adequate ventilation [56].

Code	Country	Pressure Relationship	Min. Outdoor Air Change Rate (ACH)	Min. Total Air Change Rate (ACH)	Design Air Temperature (°F)	Design Relative Humidity (%)
Patient Room/General Wards						
AIA	United States	Neutral	2	6	21 to 24	Not Specified
ASHRAE	United States	Neutral	2	6	21 to 24	30 to 60
HTM 2025	United Kingdom	Neutral	Not Specified*	Not Specified†	20 to 22	40 to 60
Intensive Care Wards						
AIA	United States	Neutral	2	6	21 to 24	30 to 60
ASHRAE	United States	Neutral	2	6	21 to 24	30 to 60
HTM 2025	United Kingdom	Neutral	Not Specified*	Not Specified†	20 to 22	40 to 60

* Minimum outdoor air (ie. fresh air) rate of 8 l/s per person specified.
†100% outdoor air encouraged.

Table 1.1: Guidelines governing the ventilation of general and intensive care ward. (Source: Clive B. Beggs, May 2008)

The above studies illustrate the importance of looking beyond air change rates and examining the effects that other factors such as supply and exhaust location, door position and motion, spatial orientation, surface composition, temperature, humidity, and air distribution patterns have on particle migration in clinical spaces. Additionally, population density, number of susceptible, length of exposure, infectious particle settling rate, number of infected people producing contaminated aerosols are important factors.

Ideally, airflows in patient rooms should be directional and laminar [23] between supply, source, and exhaust. Although the instability of free shear layer the flow discharging from supply diffuser will cause turbulence in the flow. When the exhaust is located away from the contaminant source, airflow path is influenced by nearby supply air, the source is outside of the directional airflow between supply and exhaust, contaminants migrate to other places in

the patient room [22]. Air flow velocities necessary to achieve high air change rates invariably produce turbulent airflows. Turbulent airflows associated with high air change rates may not only interfere with directional airflow within clinical spaces but may also breakdown containment control between clinical spaces [24]. Also if the central air conditioning is used in the patient rooms there might be a chance of cross-infection. A recently published empirical study [58] indicates that in some situations there may be limits to the improvements in the environment that can be achieved by increasing ACH in the occupied zones of rooms.

It is also important to understand the interaction and the role that particle size and particle transmission dynamics play in infectious disease transmission. It is generally accepted in the current mechanical engineering and medical community that particles with an aerodynamic diameter of 5 μm or less are aerosols, between 5 μm to 10 μm are droplet nuclei whereas particles of 10 μm are large droplets [22]. Studies have suggested that droplets larger than 20 μm rapidly settle onto surfaces [59], while aerosols between 0.5 and 2 μm remain in the air for long periods and are more likely to be captured in the respiratory tract and produce infection (McCluskey, Sandin, and Greene 1996). Studies show that 80 to 90 percent of particles from human expiratory activities are smaller than 1 μm [31]. Small droplets may also participate in short-range transmission, but they are more likely than larger droplets to evaporate to become droplet nuclei, at which point they have the potential for long-range airborne transmission [56]. There is substantial literature on cough droplet size distribution [28-32] and exhaled air temperature [33]. For large droplets generally with a mass median aerodynamic diameter (MMAD) of >10 micrometers and particles with MMAD <20 μm the process of disease transmission happens instantaneously. The distance droplets travel depends on the velocity and mechanism by which respiratory droplets are propelled from the source, the density of respiratory secretions, environmental factors such as temperature and humidity, and the ability of the pathogen to maintain infectivity over that distance [22].

Pathogen-laden droplets are expelled into the air by an infected person by coughing, sneezing, breathing or talking [28]. Zhu et al. (2006) [34] indicated the peak cough velocity

varied from 6 to 22 m/s with an average of 11.2 m/s or about 2000 fpm. Variations in this velocity depend on gender, individual size, and relative health status. The pathogen-laden droplets dry out and produce droplet nuclei that may be transmitted over a wide area. Cole and Cook [36] and Wells [35] report that sneezing can introduce as many as 40,000 droplets which can evaporate to produce droplets of 0.5 μm to 12 μm. Fitzgerald and Haas [37] report that a cough can generate about 3000 droplet nuclei, the same number as talking for 5 minutes. Duguid [28] notes that a single cough typically produces about 1% of the amount of droplets compared to sneezes, but coughs occur about ten times more frequently than sneezes. Normal breathing actually generates more bio-aerosols than a cough or sneeze. The particles making up aerosol in normal exhalation are less than 1 micron in size and these smallest particles are primary vectors of contagion. Experimental studies with smallpox conducted by Downie and colleagues (1965) and investigations by Yu and colleagues (2004) [61] during the 2003 global SARS outbreaks suggest that droplets from patients could reach persons located 1.83 meters (6 feet) or more from their source. Particles larger than about 0.3 μm in diameter will tend to settle out over time and these will include most bacteria, fungal spores, dust particles, and droplets or droplet nuclei, which may include clumps of viruses or bacteria. Settling causes particles to accumulate on the floor or the top side of horizontal surfaces [13]. Gregory [62] studied the terminal velocities of several fungal spores and showed a relationship between falling velocity and size. These results are shown in Figure 1.1.

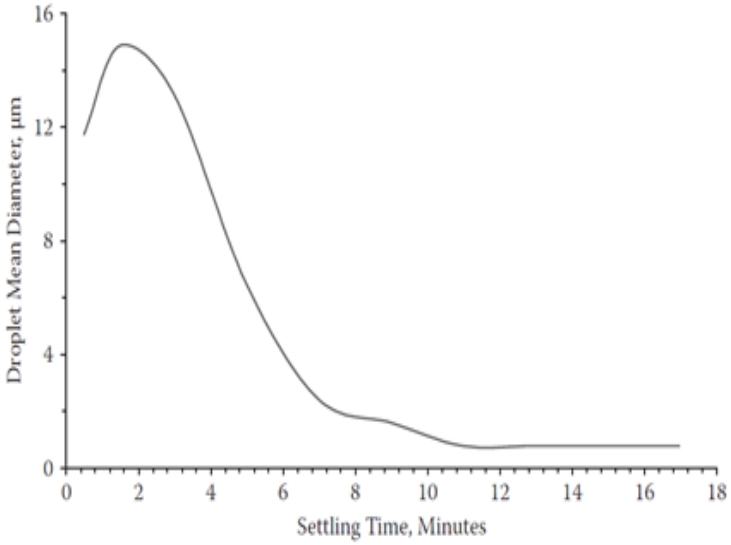

Figure 1.1: Settling time versus droplet size

The microbial composition of the air in hospitals varies between wards, and often the highest number of isolates is found in corridors, followed by operating rooms. In one study of airborne microbial contamination in the operating room and intensive care units (ICUs) of a surgery clinic, Holcatova, Bencko, and Binek (1993) measured bacterial concentrations of 150-250 CFU/m^3 (colony-forming unit) [13]. CFU is a unit used to estimate the number of viable bacteria or fungal cells in a sample. Viable is defined as the ability to multiply via binary fission under the controlled conditions. The World Health Organization (WHO) recommends not more than 50 CFU/m^3 of fungi in hospital air, over half of the facilities tested in this study exceeded this limit [52]. For bacteria, WHO recommends a limit of 100 CFU/m^3 and about 30% of facilities were beyond this limit [13]. The normal levels of requisite air filtration should completely eliminate virtually all fungal spores and environmental bacteria, and therefore the presence of these environmental microbes in the indoor air of hospitals indicates either a failure of the filters to perform or, more likely, the fact that there are alternate pathways by which such microbes may enter the hospital [13]. The table below summarizes some of the studies on hospital airborne concentrations of microorganisms [13].

Typical Airborne Concentrations of Bacteria in Hospitals		
Area	Mean Level (cfu/m^3)	Reference
General areas	55	Ross et al. 2004
General areas	80	Andrade and Brown 2003
General areas	207	Tighe and Warden 1995
General wards	31	Ekhaise, Ighosewe, and Ajakpovi 2008
Hospital room	1224	Solberg et al. 1971
ICU and critical care	83	Tighe and Warden 1995
Isolation room	314	Solberg et al. 1971
NICU	36	Kowalski and Bahnfleth 2002
Nurse's stations	52	Tighe and Warden 1995
Patient rooms	104	Tighe and Warden 1995
Ultraclean/laminar OR	1.5	Solberg et al. 1971
Ultraclean/laminar OR	7	Ritter et al. 1975
Ultraclean/laminar OR	7.7	Berg, Bergman, and Hoborn 1991
Ultraclean/laminar OR	19	Luciano 1984
Ultraclean/laminar OR	22	Friberg and Friberg 2005
Conventional OR	23	Bergeron et al. 2007
Conventional OR	24	Berg, Bergman, and Hoborn 1989
Conventional OR	28	Nelson 1978
Ultraclean/laminar OR	29	Brown et al. 1996
Conventional OR	35	Lidwell 1994
Conventional OR	65	Lowbury and Lidwell 1978
Conventional OR	74	Hambraeus, Bengtsson, and Laurell 1977
Conventional OR	74	Tighe and Warden 1995
Mean level for operating rooms	34	
Mean level for ICUs, NICUs, isolation	114	
Mean level for general areas	250	

Table 1.2: Typical Airborne Concentrations of Bacteria in Hospitals (Source: Kowalski, 2013)

It is equally important to take into account the physical position of occupants in the room. Studies have shown that the position of the "coughing" patient and the "staff" have a pronounced effect on the "staff" exposure to potentially infective particles. The posture of the coughing infected patient also has a great impact on the exposure of medical staff and other patients [38]. Exposure of the medical provider is a result of the interaction of several factors: the airflow pattern in the space, the distance between the exposed person and the sick patient, the posture of the staff etc. [39]. For a patient coughing upwards (towards the ceiling exhaust vent) contaminants were successfully exhausted and the total volume (TV) ventilation did not have as significant impact on the exposure level as in the studied case when the patient coughed sideways towards the face of the medical provider [38]. Kierat suggests that a good contaminant control solution in hospital rooms is to position the TV exhaust as close as possible to the polluting source: the sick coughing patient in this case. A similar arrangement has been suggested by others [38, 40-43].

In the context of airborne infectious agents, source control refers primarily to maintaining pressure differentials between spaces to prevent these agents from migrating between zones. The CDC [4], ASHRAE [3] and FGI/AIA [2, 5] documents contain a recommended pressure differential of +/- 2.5 Pa for pressurized areas, yet this pressure differential is not always maintained in practice. Pavelchak et al. [26] studied 82 isolation rooms in New York hospitals and identified significant problems associated with pressurized rooms; 54% of the isolation rooms were found to have a doorway airflow direction opposite of the design specifications (into the room). Unbalanced ventilation systems, shared anterooms, turbulent airflow patterns, and control system problems led to the unexpected outward directional airflow. The study also found that of the isolation rooms that had continuous pressure monitors present, 50% of them indicated pressures opposite in sign to those indicated by a smoke test. This high rate of failure highlights the need for alternative design and analysis tools [45].

Acceptable IAQ in terms of infection control can be achieved by using ventilation in conjunction with air filtration on recirculated and fresh air, mechanical arrestance media to

clean air of microbial and other particulate matter; and irradiation in targeted applications, using ultraviolet germicidal irradiation (UVGI) to alter airborne and surface-borne microbes and limit the proliferation of the infectious agents [22].

Filtration is a primary method used in hospitals to remove airborne pathogens. ASHRAE Standard 170 [3] currently requires two levels of filtration for patient rooms other than protective environment rooms: a MERV 7 pre-filter and a MERV 14 secondary filter. Protective environment areas are required by the standard to have HEPA filtration for supply air, corresponding to removal of at least 99.97% of 0.3 μm particles at the rated flow. Similarly, negative pressure areas that recirculate air (only allowed if rooms are retrofitted from standard patient rooms and it is impractical to exhaust directly outdoors) are required by Standard 170 to have HEPA filtration on the return air inlets [45]. HEPA filters do not necessarily remove all microbes, and it is possible that some microbes in the most penetrating particle size range ($<$3 μm) of a HEPA could penetrate the filter in small numbers [25].

Ultraviolet germicidal irradiation (UVGI) is intended to limit transport of infectious agents from patient rooms in hospitals or lobbies in public access buildings by reducing their airborne levels [63]. There are three types of UVGI systems: irradiation of the upper zones of occupied spaces (called upper-level room), in-duct and in-room. In-duct and in-room UVGI systems may be used in operating rooms or hospital waiting rooms. In-duct UVGI systems use banks of UV lights within the duct system in order to inactivate microbes. Upper-level room UVGI relies on room air motion to transfer pathogens to UV lights that are suspended from ceilings and shielded to prevent UV exposure to occupants. In-room UVGI uses a combination of fans and UVGI in recirculating units. While UVGI has existed for over fifty years, research regarding its effectiveness in healthcare facilities is still limited and more evaluation and demonstration work is needed. The effectiveness of in-room UVGI depends on the mixing effectiveness of the ventilation system, which determines the cumulative dose of irradiation experienced by the pathogens [64]. Well-mixed room models neglect this important aspect of UVGI system performance; thus, computational fluid dynamics (CFD)

programs have been used to obtain a more detailed understanding of their effectiveness. Noakes et al. used both analytical and CFD methods to model UVGI. This study found that multi zonal analytical models, which subdivide rooms into vertical levels, can provide zonal concentrations that compare well to CFD simulations [63]. Another CFD study of UVGI [9] found that UVGI does not kill a significant portion of viable airborne particles. However, the authors felt that the CFD parameters used in the study resulted in an unrealistically high fraction of removal by deposition. High air change rates can also decrease UVGI effectiveness by decreasing particle residence time in the UV zone, as shown in a CFD modeling study done by Memarzadeh et al. [12]. Kowalski et al. [30] define UVGI effectiveness in terms of kill rates, which are comparable to filter efficiencies [45]. In order to model UVGI deactivation of airborne pathogens, the authors assigned URV (Ultraviolet germicidal irradiation Rating Value) to levels of UV intensity, analogous to MERV filter ratings. The URV and MERV removal fractions for several airborne pathogens were computed and combined, creating a single MERV/URV removal efficiency. For example, a pathogen removal system that employed an URV8 UVGI system with a MERV 8 filter was assigned a removal efficiency of 0.19 for influenza. Further study of UVGI is still needed to understand its effectiveness and to develop engineering design guidance [63].

Dilution ventilation with fresh air becomes critical for airborne infection control whenever infectious and susceptible people share airspace without the use of particulate respirators, such as in waiting rooms, outpatient clinics, emergency departments, shared wards, and investigation suites. These spaces are often ventilated at levels well below those recommended for the control of TB transmission. In resource-limited settings lacking negative-pressure respiratory isolation, natural ventilation by opening window is recommended for the control of nosocomial TB [79], but the rates and determinants of natural ventilation in healthcare facilities have not been defined. There is little to no research on the effect on health outcomes in hospitals with operable windows, though theoretically, operable windows would avail the room occupant with smells, breezes and all the sensory stimuli of an open environment. In

addition, advocates of sustainable design argue that natural ventilation can increase energy efficiency on buildings as well as improve indoor environmental conditions. A recent study of an acute care hospital in two California climates found that increased daylighting with daylight controls reduced overall energy use by approximately 10%, with hybrid natural ventilation contributing another 10%. Although for many the primary motivation to increase daylighting is to achieve its benefits for patients and staff-especially that of connection to the world via operable windows- energy and resiliency benefits should not be discounted [80].

A comprehensive literature review by Li and colleagues (2007) [65] of 40 studies found 10 studies that were conclusive and 12 studies that were partly conclusive in favor of the relationship between ACH and airborne transmission. Among the 10 conclusive studies, several showed an association between airflow patterns and the spread of diseases (Bloch et al. 1985; Gustafson et al. 1982; Hutton et al. 1990; Wehrle et al. 1970), including several that examined clusters of SARS-CoV (Li et al. 2005; Yu et al. 2005; Wong et al. 2004). Infectious agents included in this review also involved the measles, Mycobacterium tuberculosis, chickenpox, influenza, smallpox, and cold viruses. These 10 studies demonstrated the role of building ventilation and airflows in relation to the spread or control of airborne infectious diseases. However, data were insufficient to specify or quantify the minimum ventilation requirements in the hospital and non-hospital environments in relation to the spread of airborne infection. One exception is the work of Menzies and colleagues (2000), which showed an association between tuberculin conversion and ventilation of general or non-isolation patient rooms of less than 2 ACH [56].

Energy efficiency also plays an important role in the healthcare system. Today, operational hospitals in the U.S. consume an enormous amount of energy. All buildings account for 50% of energy consumption; the remainder is consumed by transportation and industry in the United States [54]. Healthcare buildings account for less than one percent of all commercial buildings, and two percent of all commercial floor space, yet account for 5.5% of commercial building energy consumption. And 52% of their annual energy costs is

for heating/cooling/ventilation [55]. More recent findings by the University of Washington Integrated Design Lab (UW IDL), as reported in a 2009 American Society of Healthcare Engineering (ASHE) paper, compare energy used by hospitals in the Pacific Northwest region of the United States to those in Norway and Sweden. To generalize, United States hospitals use about twice the amount of energy as Norwegian hospitals and about four times the amount used in Swedish hospitals. A short list of methods that some of these Scandinavian hospitals employ includes severely limiting re-heat, reducing air change rates, using displacement ventilation in combination with radiant heating and cooling, recovering heat from all internal heat sources, and relying on ground-source heat pumping for the majority of additional heating and cooling needs [53].

Additionally, increasing or decreasing ventilation rate by as little as one air change per hour in an average size isolation room can result in a difference of $150 to $ 250 per year in heating and cooling costs [22]. Conditioned ventilation air can cost $4 to $8/cfm/year, which is a substantial cost for large biomedical facilities that use high air-exchange rates to maintain healthy environments. Increasing the air exchange rate of a typical 70-square-meter laboratory from 6 ACH to 14 ACH can increase the annual heating, ventilation, and air conditioning (HVAC) energy cost by around $8,000 [56].

To validate the findings of these and other similar studies, a series of experimental tests were conducted in an actual hospital using a sonic anemometer to observe the effectiveness of air change rates and flow pattern with mechanical ventilation to contain, dilute, and remove respiratory aerosols in patient rooms designed for mechanical ventilation. This study also validates the use of sonic anemometer for indoor use.

CHAPTER 2

Method

2.1 Gill Instrument's WindMaster Model 200-1590-PK-020/W

Gill Instrument's WindMaster Model 200-1590-PK-020/W:

For this study, we used a company calibrated 3D sonic anemometer, WindMaster (Figure 2.1) as described in specifications (Table 2.1) to obtain airflow speed and direction due to the forced convection in the patient room. Direction sensitivity of WindMaster was verified by smoke pen and also airflow rates were compared with Shortridge flow meter.

The WindMaster measures the time taken for an ultrasonic pulse of sound to travel from an upper transducer to the opposite lower transducer and compares it with the time for a pulse to travel from lower to the upper transducer.

Likewise, times are compared between each of the other upper and lower transducers. As Figure 2.3 shows, the air velocity along the axis between each pair of transducers can then be calculated from the times of flight on each axis. This calculation is independent of factors such as temperature. From the three-axis velocities, the wind speed is calculated, as either signed U, V, and W or as Polar and W. The acoustic path length for each transducer pair is 15cm.

Figure 2.1: Gill WindMaster 3D Sonic Anemometer Model 200-1590-PK-020/W

It can be seen from Figure 2.9 that the speed of sound in air can be calculated from the times of flight. From this, the sonic temperature can be derived from the formula,

$$TS1 = C1^2/403 \tag{2.1}$$

Where,

TS1 = Sonic temperature

C1 = Speed of sound

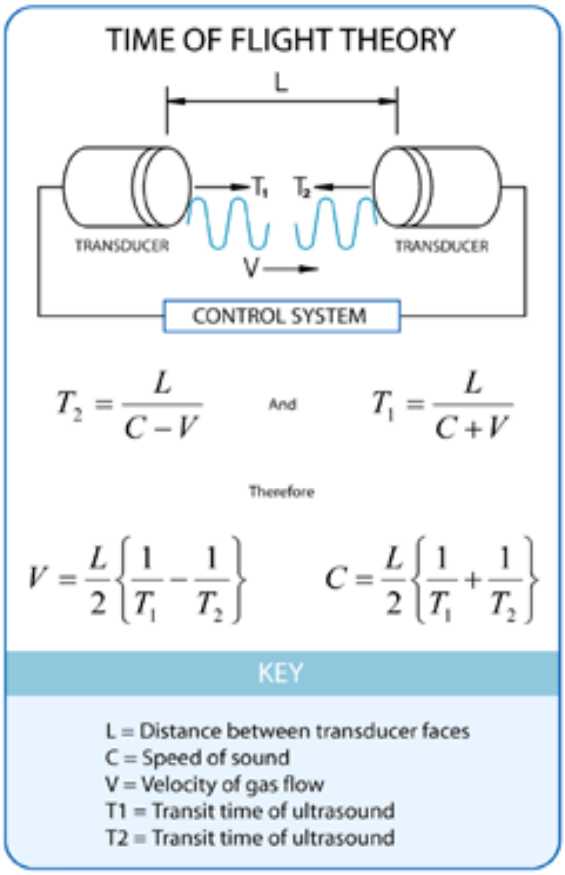

Figure 2.2: Time of Flight Details

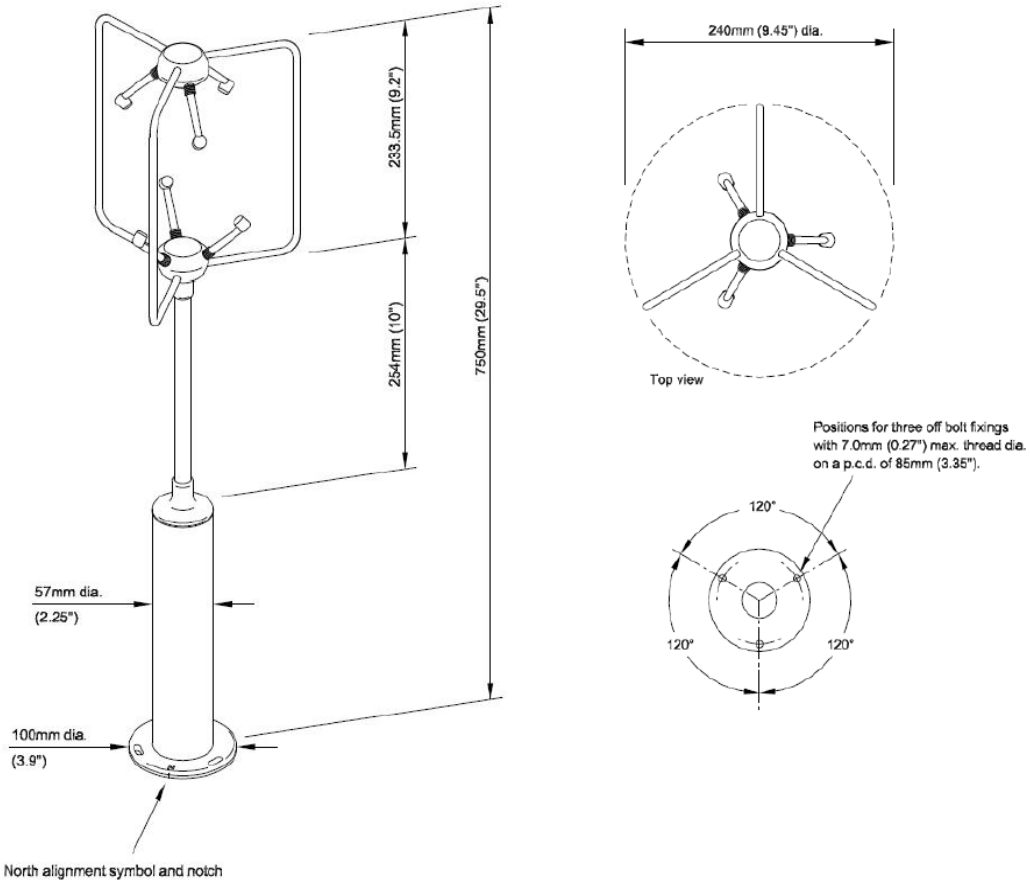

Figure 2.3: North Spar Alignment and Dimensions

U, V, and W axes definition:

+U is defined as towards the direction in line with the north spar as indicated in the diagram. +V is defined as towards the direction of 90°anti-clockwise from N / the Reference spar. +W is defined as vertically up the mounting shaft [66].

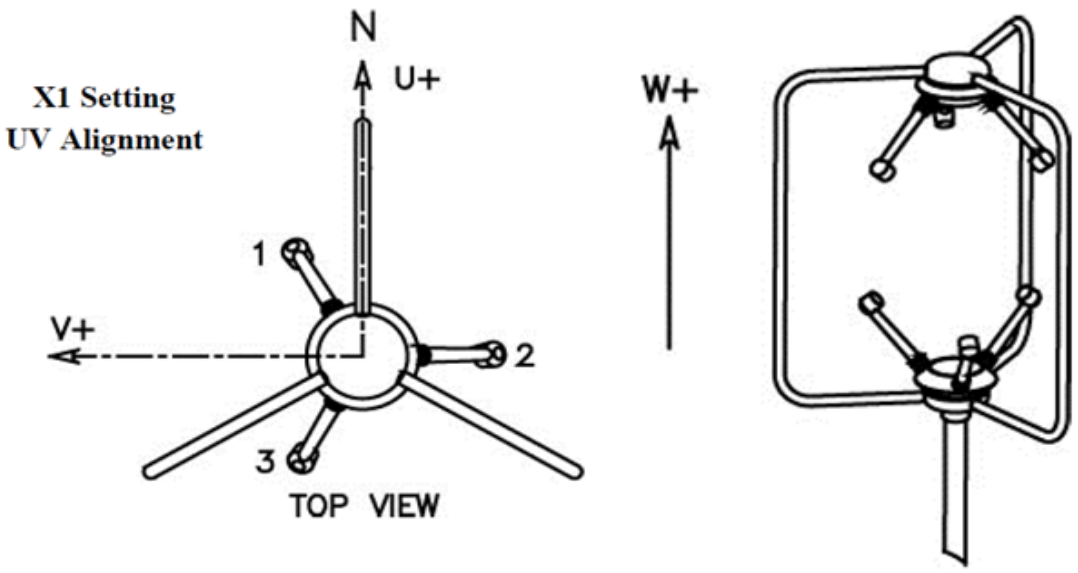

Figure 2.4: U, V and W Axis Definition

WindMaster Specifications:

Wind Speed Specifications	
Range	0-50m/s
Accuracy*	<1.5% RMS @ 12m/s
Accuracy*	<1.0% RMS @ 12m/s (custom)
Resolution	0.01m/s
*accuracy applies forwind speed and for wind incidence up to ±30°from the horizontal	
Wind Direction Specifications	
Range	0-359°
Accuracy	2°@ 12m/s
Accuracy	0.5°@ 12m/s (custom)
Resolution	0.1°
Sonic Temperature	
Range	-40°C to +70°C
Resolution	0.01 °C

Accuracy	-20°C to +30°C within ±2°C of ambient temperature
Speed of Sound	
Range	300- 370m/s
Resolution	0.01 m/s
Accuracy	< ±0.5% @ 20°C
Measurement	
Internal Sample Rate	20Hz (32Hz optional)
Output Rates	1, 2, 4, 8, 10, 16, 20 Hz (32Hz option)
Units of Measure	m/s, mph, kph, knots, ft/min
Output Formats	UVW, Polar
Averaging	Flexible 0-3600 s
Digital Output	
Communication	RS232, 422, 485
Baud Rates	2400 - 115200
Format	ASCII
Analogue Outputs (Optional)	
Resolution (12 or 14 bits)	4 channels available
Selectable Range	User selectable full-scale wind speed
Output Type	0-20mA, 4-20mA, 0-5V, ±2.5V, ±5V
Analogue Inputs (Optional)	
Resolution (12 or 14 bits)	Up to 4 single ended or 2 differential
Input Type	±5V
Power Requirement	
Anemometer	9-30V DC (55mA @ 12V DC)
Mechanical	

Weight	1.0 Kg
Size	750mm x 240mm
Environmental	
Protection Class	IP65
Humidity	<5% to 100% RH
Operating Temperature	-40°C to +70°C
Precipitation	300mm/hr
EMC	Emissions BS EN 61000-6-3 Immunity BS EN 61000-6-2

Table 2.1: WindMaster Specifications (Source: Gill Instruments Limited, 2010)

2.2 Shortridge Flow Meter ADM-880C

The ADM-880C AirData multimeter measures air velocity, temperature, pressure, and airflow. During velocity or flow readings, the meter automatically measures the local temperature and barometric pressure and corrects for local air density [67].

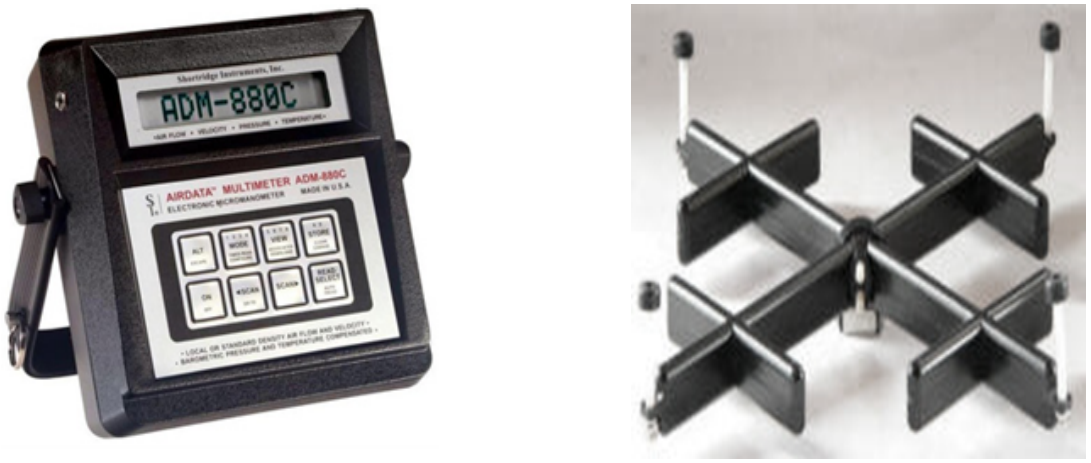

(a) (b)

Figure 2.5: Shortridge Flow Meter ADM-880C

Specifications:

Specifications	
AIR VELOCITY	±3% of reading ±7 fpm from 50 to 8000 fpm pitot tube (30,000 fpm FS); 50 to 5000 fpm AirFoil; 50 to 2500 fpm VelGrid.
DIFFERENTIAL PRESSURE	±2% of reading ±0.001 in wc from 0.0500 to 50.00 in wc, (0.0001 to 60 in wc FS); 20 psid safe pressure.
TEMPERATURE	±0.5°F accuracy from 32°F to 158°F using ADT440 Series Temp Probes (-67°F to 250°F FS); 0.1°F resolution.
AIRFLOW	Accuracy is ±3% of reading ±7 cfm from 100 to 2000 cfm; range is 25 to 2500 supply, 25 to 1500 exhaust with 8400 FlowHood.
ABSOLUTE PRESSURE	±2% of reading ±0.1in Hg from 14 to 40 in Hg referenced to vacuum. 60 psia maximum safe pressure.

OPERATIONAL TEMPERATURE LIMITS	40°F to 140°F.
AIR DENSITY CORRECTION	Local or standard (mass flow) air density correction range is 14 to 40 in Hg and 32°F to 158°F.
POSITION SENSITIVITY	Unaffected by position.
MEMORY	2000 readings, sequence labeled, sum and average, minimum, maximum, and standard deviation for each mode.
CALIBRATION	Calibration certified NIST traceable.
READOUT	10 digit, 0.4", high contrast, liquid crystal display
METER HOUSING	6.0" x 6.4" x 2.7" high impact ABS. 36 oz
CONNECTIONS	1/4" OD slip-on for 3/16" ID soft tubing.
BATTERY LIFE	3000 readings per charge, 500 recharge cycles.

Table 2.2: Shortridge Flow Meter ADM-880C Specifications (Source: Shortridge Instruments, Inc., 2008).

2.3 Patient Room Geometry

The experiment was conducted in an actual patient room with the window facing south and located in third floor of hospital at Meridian, ID. Figure 2.8 shows the location of the patient bed, seating area, furniture, supply and return air locations, the position of the door to the corridor and bathroom and window position. The exhaust fan in the bathroom was kept ON during the experiment. The flow rate from the bathroom exhaust fan was 0.080 m/s. The area of the patient room is 18.20 m^2 (196 ft^2) and the opening area of the door and window is 2.6 m^2 (28 ft^2) and 2.23 m^2 (24 ft^2) respectively. The height of the room is 2.84m (9'4"). The area of the bathroom is 6.14 m^2 (66 ft^2). Thermostat in the room was kept at 21.667°C during the experiment. The sonic anemometer measurements were taken at the same time everyday to ensure the outdoor conditions were same. The room contains several pieces of heat generating equipment including monitor, television, lights, and computer. As per ASHRAE 90.1-2010, the total sensible heat from these devices is assumed to be 22.39 W/m^2 (2.08 W/ft^2). The average solar gain of the room is calculated from EnergyPlus simulation and is 164 W (73 W/m^2). The equipment heat gain and solar gain values were calculated in order to model this experiment in computational fluid dynamics in future. The ventilation air was supplied through one ceiling mount grill diffuser (1' X 2') (Figure 2.9a) and return through one 3 way ceiling mount diffuser (2' X 2') (Figure 2.9b). Supply grill and return diffuser were installed in reverse way as per normal construction practices. As per ASHRAE 170, patient room supply outlet design should be as per group A, D or E. Group E includes ceiling diffusers, linear grilles, sidewall diffusers and grilles, and similar outlets mounted or designed for vertical downward air projection. Pressure and flow rate from the supply, return and exhaust were also measured in the patient room and corridor along with velocity and temperature with the help of a Shortridge flow meter ADM 880C instrument and Gill Instrument's WindMaster model 200-1590-PK-020/W. The flowrate measurements verified that the return air (92.32 l/s) exceeds supply air (47 l/s), producing 6 air change

per hour, and, a negative air pressure relationship with respect to the corridor. This study includes the effect of moving people and furniture in the patient room on airflow pattern. MATLAB R2017a software was used to process the air velocity data. Outdoor weather conditions were recorded from National Oceanic and Atmospheric Administration (NOAA) website.

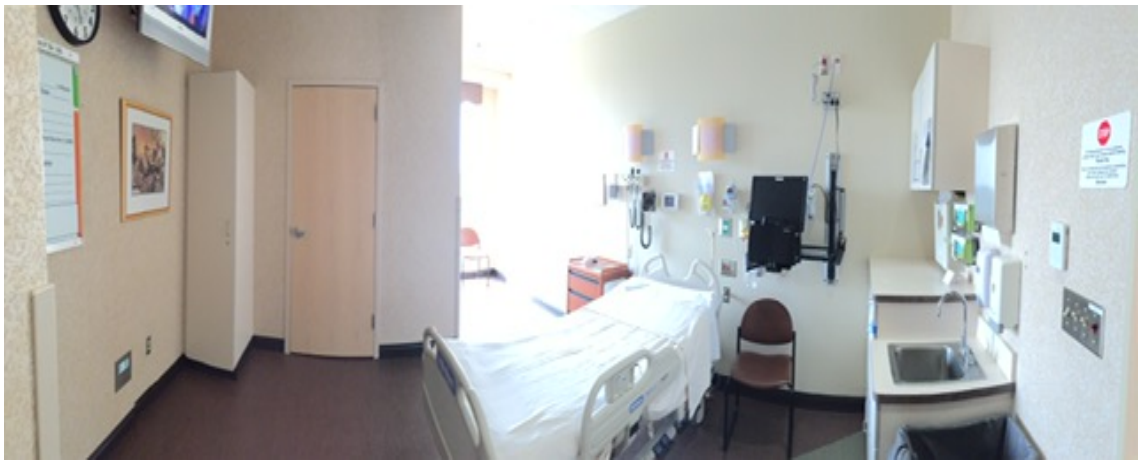

Figure 2.6: Patient Room

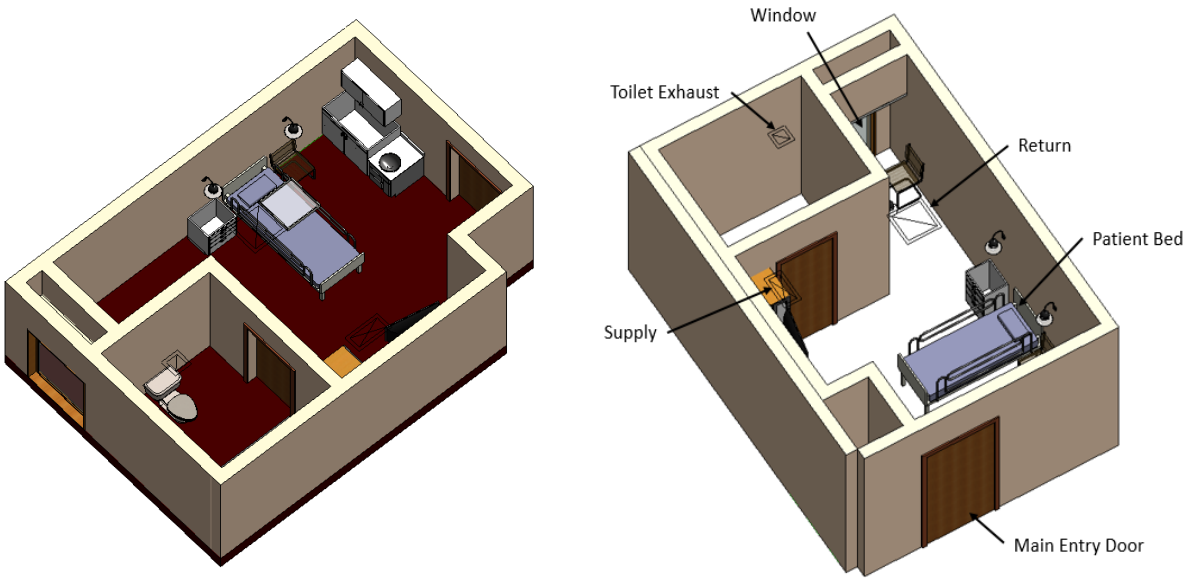

(a) (b)

Figure 2.7: Patient Room model in Revit

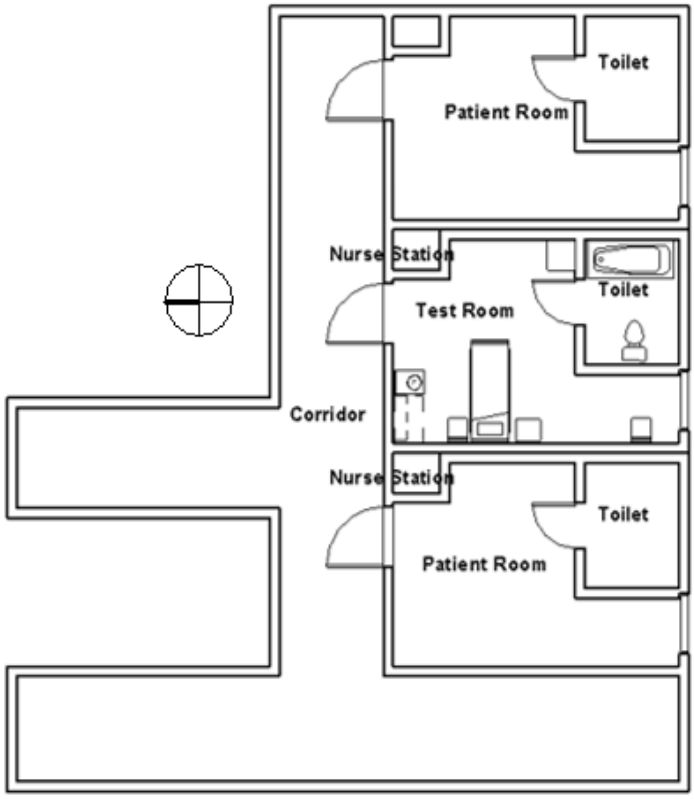

Figure 2.8: Layout of the Patient Rooms, Corridor and Nurse Stations.

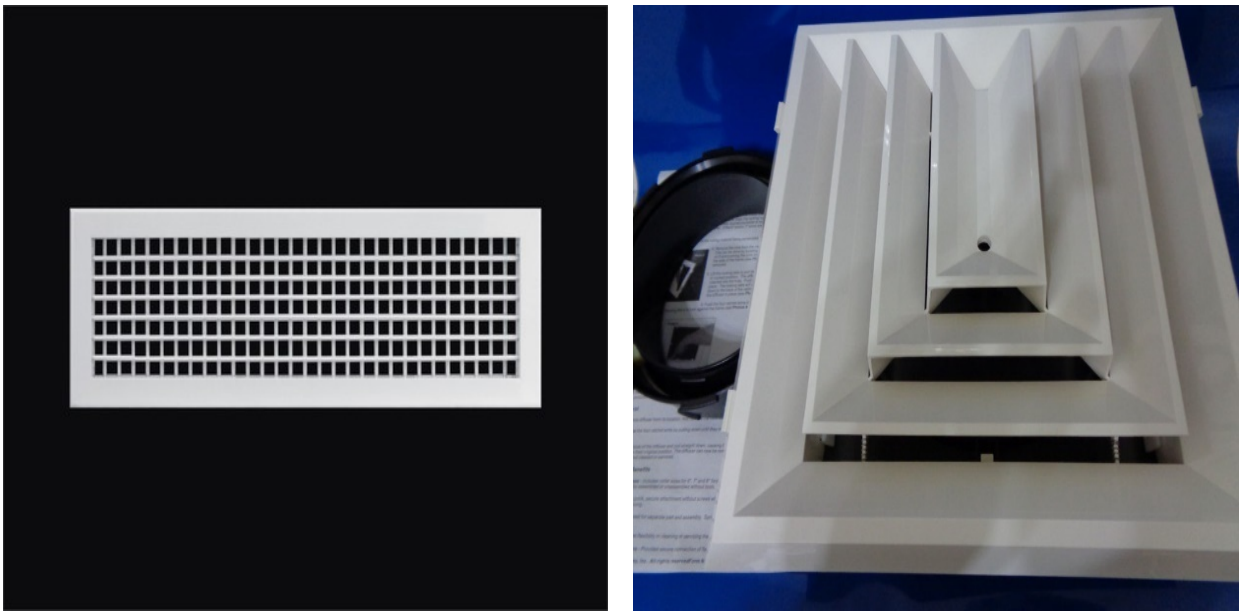

(a) Supply Diffuser (b) Return Diffuser

Figure 2.9: Supply and Return Air Diffuser Locations

2.4 Instrument Setup

The sonic anemometer head was mounted on a tripod for ease of transport and leveled after any change in sampling location (Figure 2.10). For all the tests anemometer was attached to the stand. For measurements at 4ft to 9ft the anemometer was oriented vertically and for measurements at 0.5in to 3ft it was oriented vertically but facing downwards. A bubble level was placed on the top of the instrument to set and check the vertical orientation. Instrument height was adjusted so that the center of the sensor head was at 1ft to 9ft from the floor. The measurements of the air velocity were taken on a horizontal plane at 0.5 ft., and at a 1ft to 9ft distance at increments of 1ft. above the ground. Batteries are used to power the instrument. The output of the anemometer is connected to the serial port of a computer and code was written in Processing 2.2.1 software to log the data from the anemometer. Every sample consists of 60 individual measurements.

Figure 2.10: WindMaster Setup

2.5 Data Acquisition

Processing 2.2.1, a computer software program written by Ben Fry and Casey Reas, graduate students at the MIT Media Lab within John Maeda's Aesthetics and Computation research group, was used to record three-axis sonic anemometer data. All data was then transferred to a Microsoft Excel spreadsheet for analysis. The data sampling rate for all tests with this instrument was one sample/second, and the duration of each test was 30 sec to 1 minute. The average reading at each point was calculated in a spreadsheet and then plotted using MATLAB.

2.6 Test Procedure

Before taking data in a patient room, a test measurement was taken in one of the meeting rooms at the University of Idaho's Integrated Design Lab, Boise, ID. The layout of the meeting room is shown in figures 2.11 and 2.12.

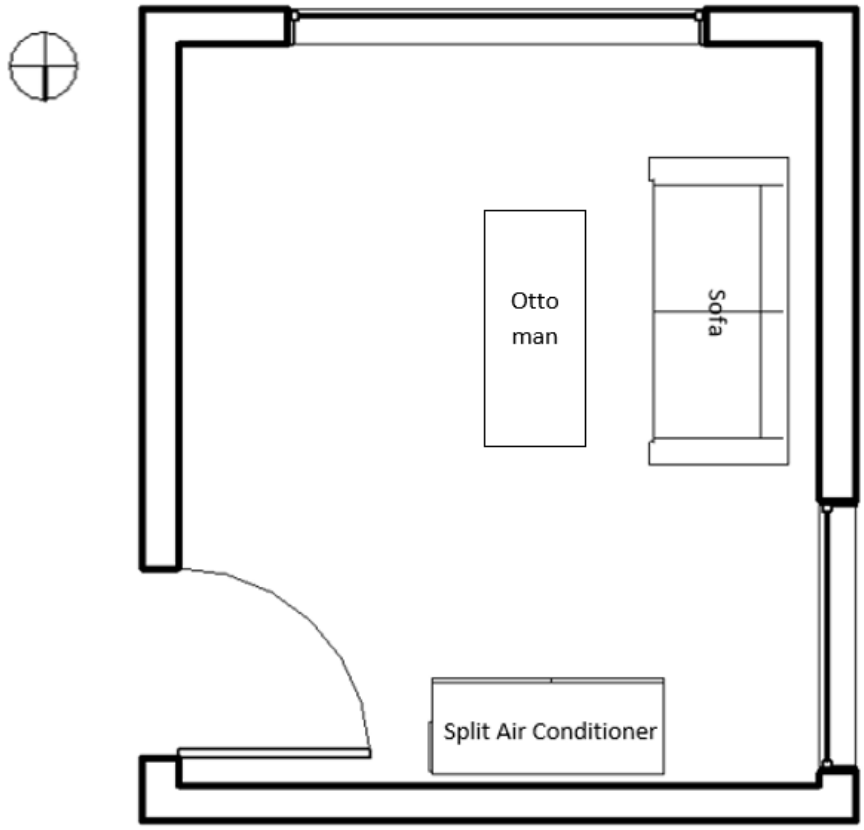

Figure 2.11: Top view of Meeting Room at Integrated Design Lab

Figure 2.12: Meeting Room

The room is oriented north-south. The room has one south facing window and one west facing window. Figure 2.11 shows the location of the furniture, split air conditioner location, the position of the door to another meeting room and window position. The area of the room is 15.24 m^2 (164 ft^2) and the opening area of the door is 2.28 m^2 (24.5 ft^2) and the windows are 6.3 m^2 (67.72 ft^2) and 1.63 m^2 (17.5 ft^2). The height of the room is 2.44 m (8 ft.). The average solar gain of the room is 225 W (765.83 Btu/hr). Pressure and indoor construction were also measured in the meeting room and corridor along with velocity and temperature with the help of Shortridge air flowmeter. A total of 840 measurements were taken at each horizontal plane at distance of 0.3 m X 0.3 m (1ft X 1ft) (Figure 2.13). Each profile consists of 168 points, separated by a uniform vertical distance of 0.30 m (1ft). At each point, the sonic anemometer measured at a sampling rate of 20 Hz during a period of 30-60 sec. Air supplied from the split AC is 1.55 m/s (305 fpm). The room has zero ventilation rate. Air from the room is drawn into the unit from the upper side of the unit and then recirculated back into the room. The vector plot below (Figure 2.14) shows the air distribution in the IDL meeting room.

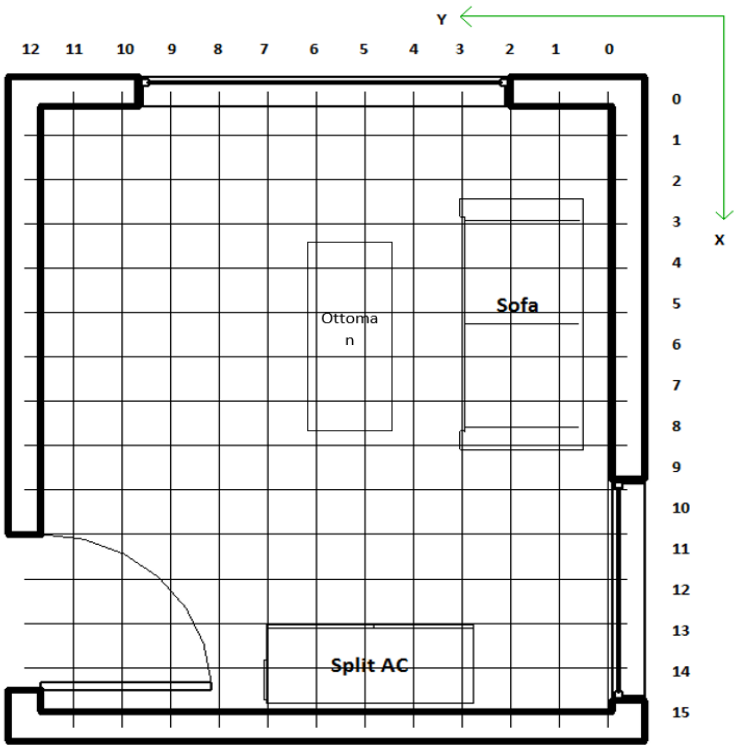

Figure 2.13: Layout of Meeting Room showing grid points 0.3m X 0.3m

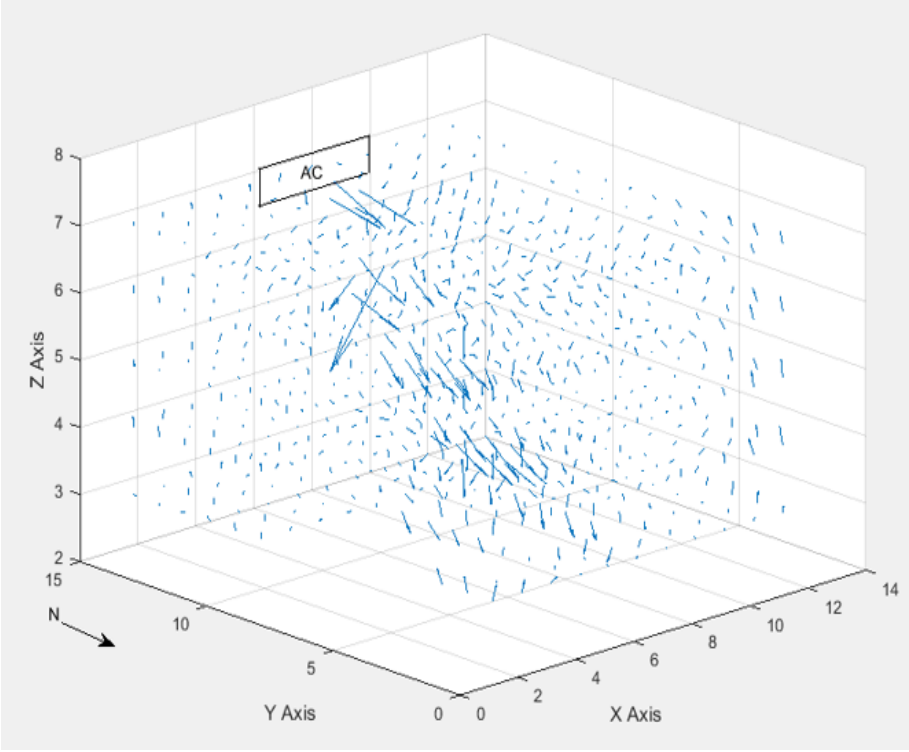

Figure 2.14: 3D resultant air velocity vectors in Integrated Design Lab's Meeting Room

The average wind speed is 0.16 m/s and the direction of the wind is North-East to South-West. Length of the blue arrow indicates the wind speed. The lowest wind speed is 0.016 m/s and the highest wind speed is 2.26 m/s. All the velocity vector figures were auto scaled to factor 0.9 using quiver command in MATLAB software.

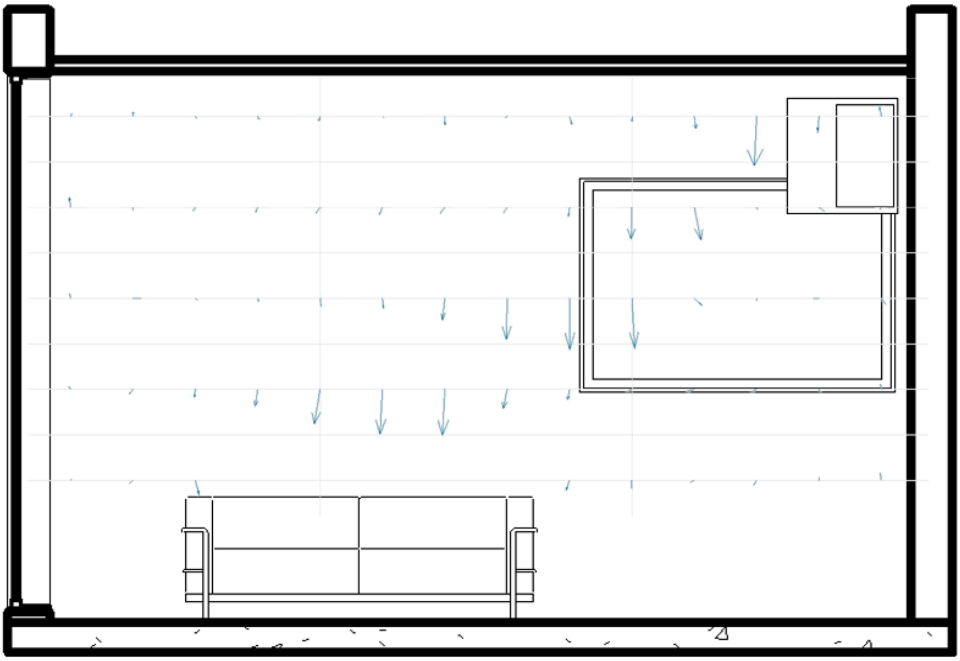

Figure 2.15: Approximate representation of two-dimensional resultants of air velocity in the YZ plane near Split Air Conditioner at Y=6

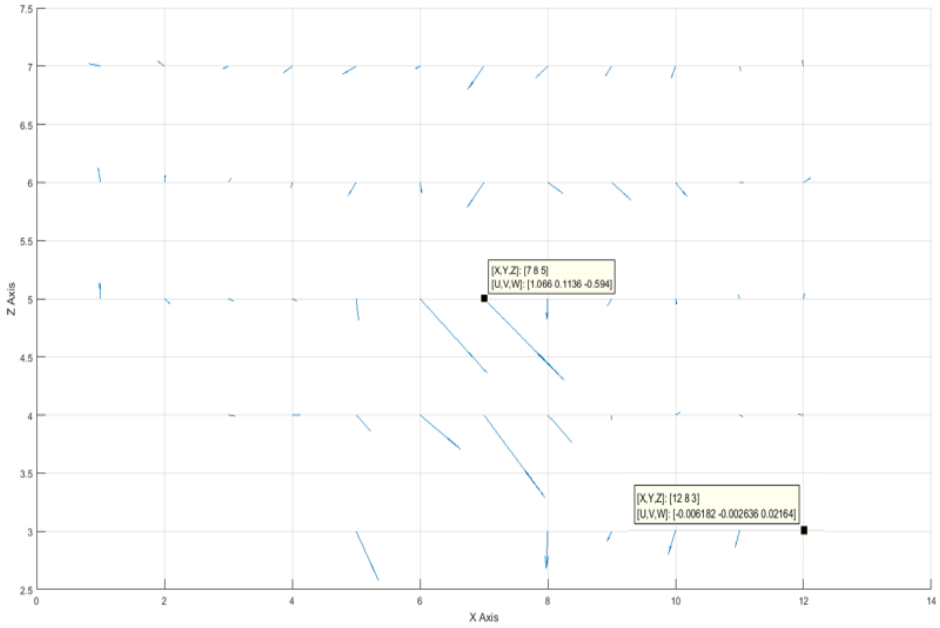

Figure 2.16: Two-dimensional resultants of air velocity in the XZ plane near Split Air Conditioner at X=8

In the above figure 2.16, data label show highest and lowest velocity in XZ plane at X=8. Highest velocity is measured in this figure was 1.225 m/s at (7, 8, 5) and lowest velocity measured was 0.0226 m/s at (12, 8, 3).

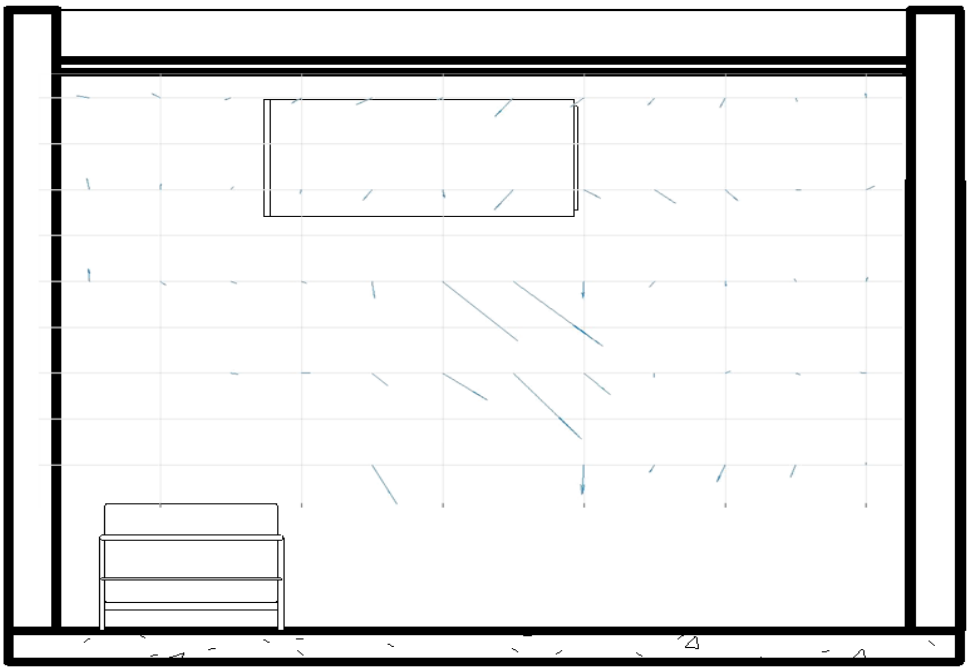

Figure 2.17: Approximate representation of two-dimensional resultants of air velocity in the XZ plane near Split Air Conditioner at X=8

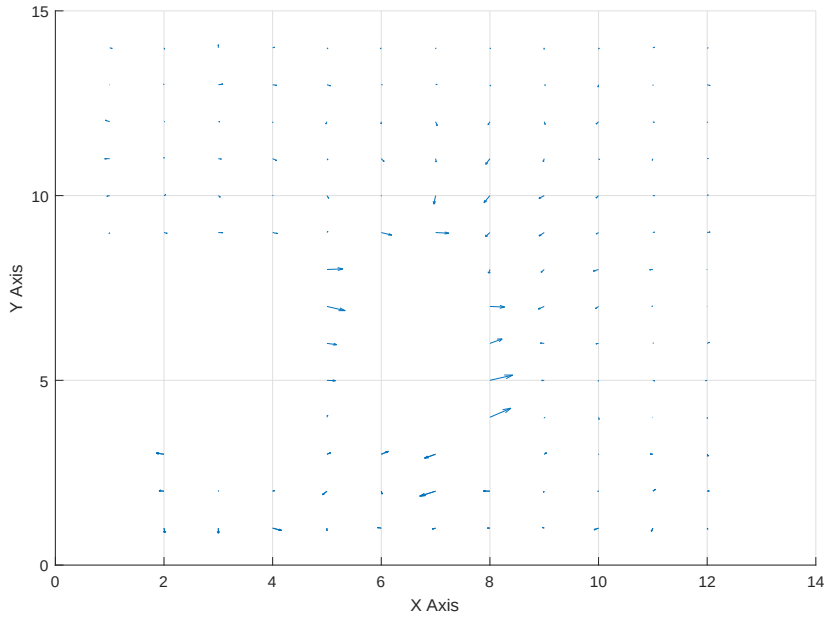

Figure 2.18: Two-dimensional resultants of air velocity in the XY plane at 3ft height above ground

Figure 2.18 show velocity vector at 3ft above ground. The blank spaces in the graph

show location of the furniture. The air flow (Figure 2.15, 2.16 and 2.17) in meeting room was downwards because of high supply fan speed in the split AC. Due to natural convection air flow near the windows and walls was upwards. Air supplied by the split air conditioner was cold and with highest fan speed. Air near the ceiling flows towards split AC and then goes back into the split air conditioner.

CHAPTER 3

Results

3.1 Airflow Patterns

In this section, the data on the velocity vectors and turbulence intensity are presented. The vector plots below (Figures 3.2 to 3.21), show the air distribution. The maximum velocity calculated is 0.55 m/s and minimum is 0.004 m/s. The temperature is in the range of 21.67°C to 22.77°C (71°F to 73°F). The outdoor climatic conditions during this experiment are summarized in Table 3.1.

A total of 2216 measurements were taken at each horizontal plane at a distance of 0.3 m X 0.3 m (1ft X 1ft) (Figure 3.1). Each profile consists of 264 points, separated by a uniform vertical distance of 0.30 m (1ft). At each point, the sonic anemometer measured at a sampling rate of 20 Hz during a period of 30-60 sec.

Dates	Average Outdoor Temperature in daytime	Average Wind Speed in daytime	Average Humidity in daytime
	(F)	(MPH)	(%)
8/23/2017-9/5/2017	95	18	32

Table 3.1: Outdoor Conditions from NOAA Website

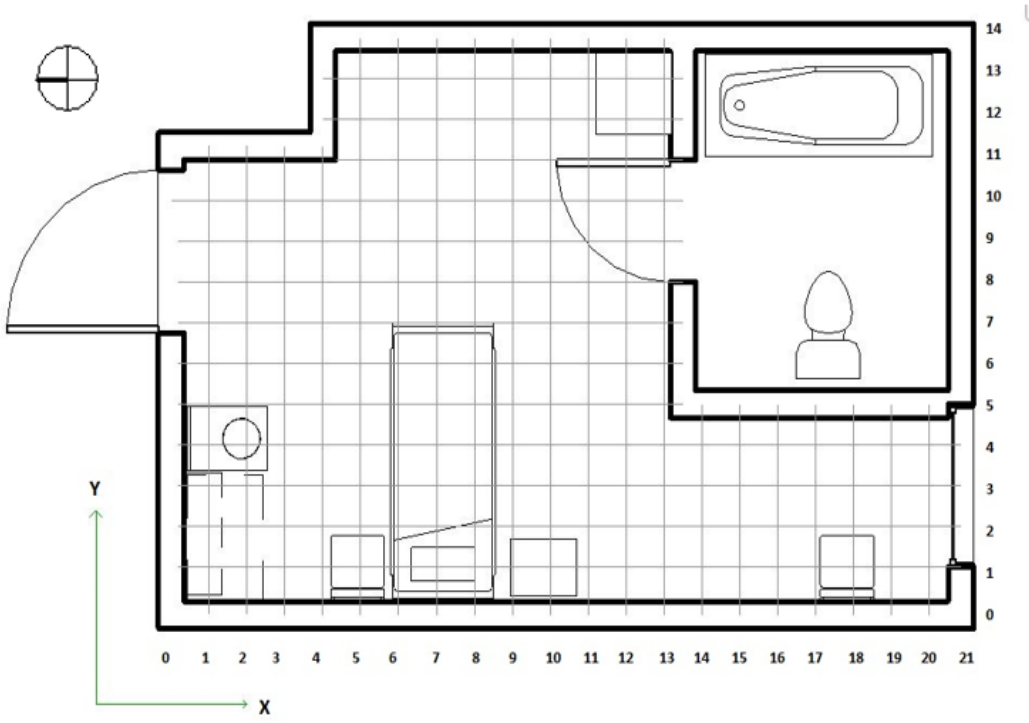

Figure 3.1: Layout of Patient Room showing grid points 0.3 m X 0.3 m

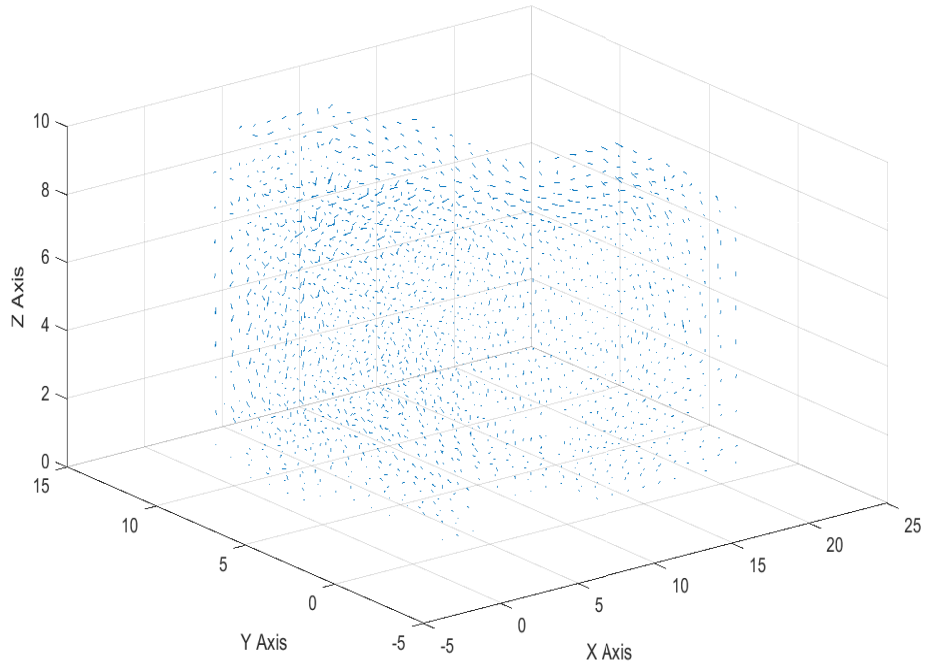

Figure 3.2: 3D resultant air velocity

The average wind speed was 0.1 m/s and the direction of the wind is North-East to South-West. Length of the blue arrow indicates the wind speed. The lowest wind speed was 0.004 m/s and the highest wind speed is 0.55 m/s. The highest velocities were registered at locations close to the inlet and exhaust registers.

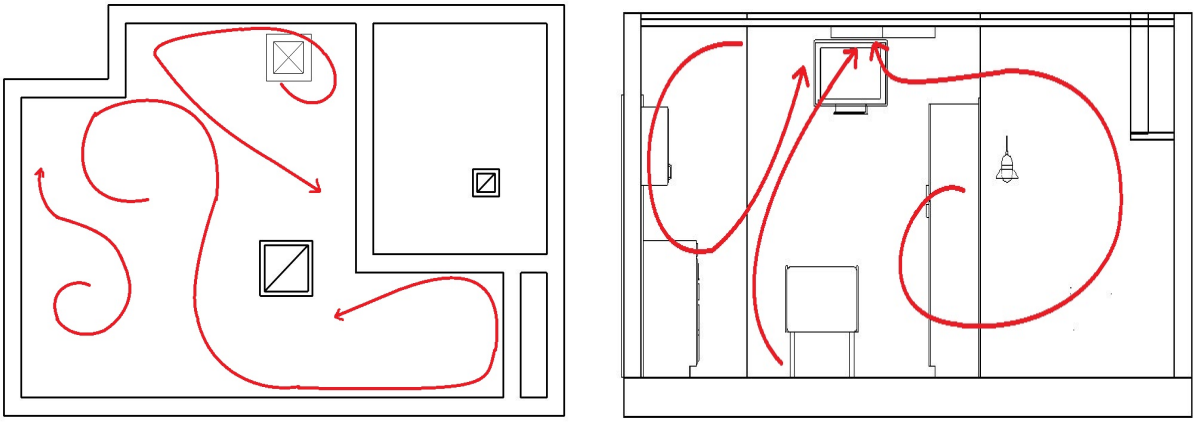

(a) Approximate representation of the inside airflow in horizontal plane at Z=5

(b) Approximate representation of the inside airflow in vertical plane at Y= 3

Figure 3.3: Approximate representation of the inside airflow

Typical results from the patient room, in the form of projections of the appropriate air-velocity vector components on different room planes: the vertical Y-Z components projected on the central plane at x=8ft, the vertical X-Z components projected on the central plane at y=3ft, 6ft, 13ft and the horizontal X-Y-component at z=0.5ft, 4ft, 5ft and 6ft, are presented in figures below (Figures 3.4 to 3.21). The absolute air velocity values, as calculated with below Equation 3.1,

$$V = \sqrt[2]{u^2 + v^2 + w^2} \tag{3.1}$$

As expected, the highest velocities were registered at locations close to inlet and exhaust registers.

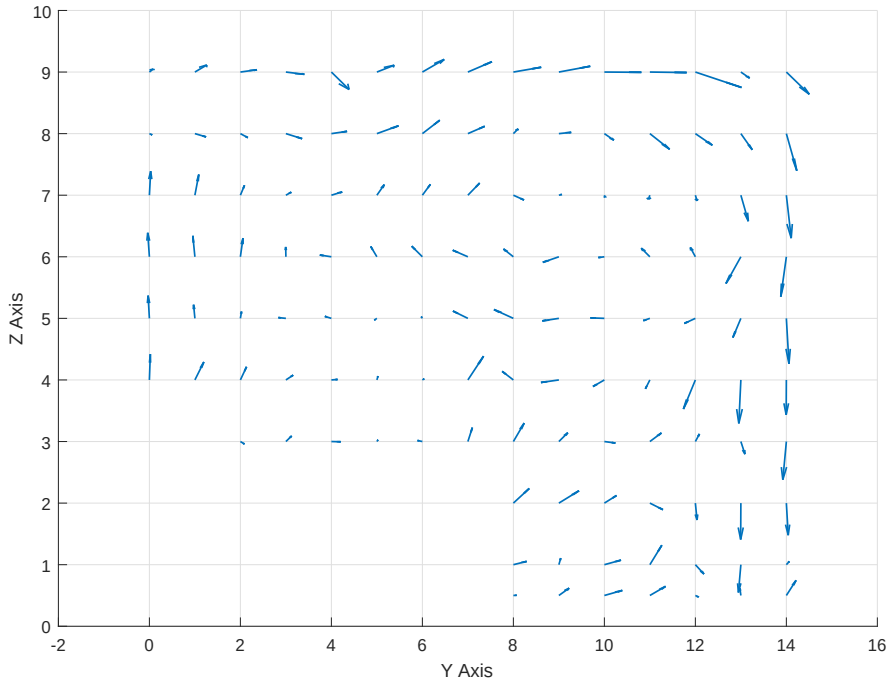

Figure 3.4: Two-dimensional resultants of air velocity in the YZ plane over the patient bed at x=8

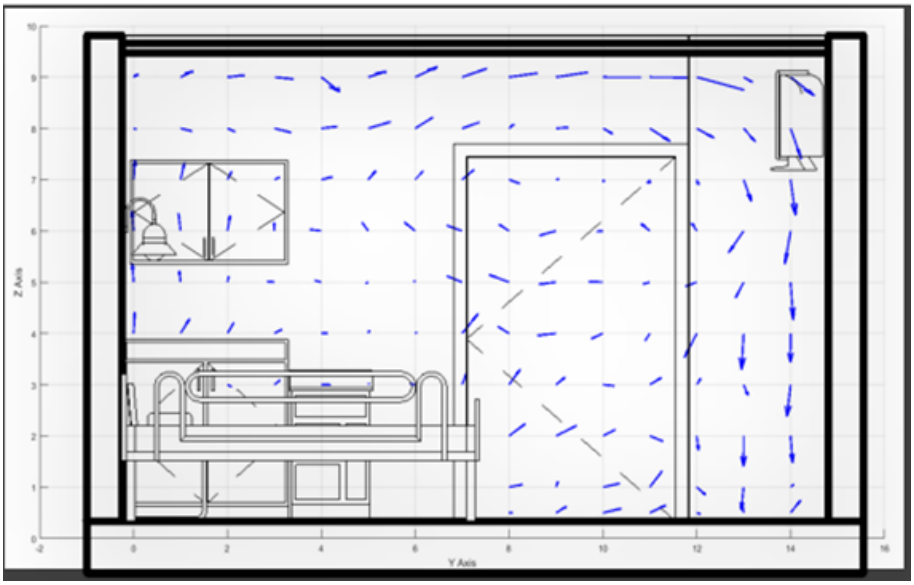

Figure 3.5: Approximate representation of two-dimensional resultants of air velocity in the YZ plane over the patient bed at x=8

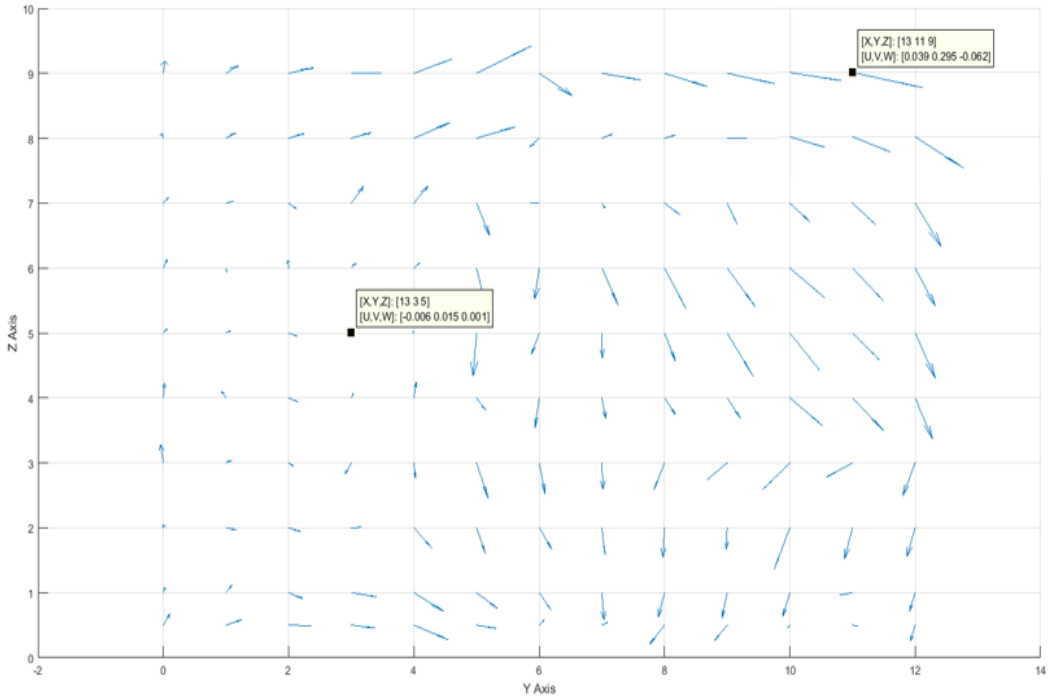

Figure 3.6: Two-dimensional resultants of air velocity in the YZ plane at x=13

In the above figure 3.6, data label show highest and lowest velocity in XZ plane at X=8. Highest velocity is measured in this figure was 0.303 m/s at (13, 11, 9) and lowest velocity measured was 0.0162 m/s at (13, 3, 5).

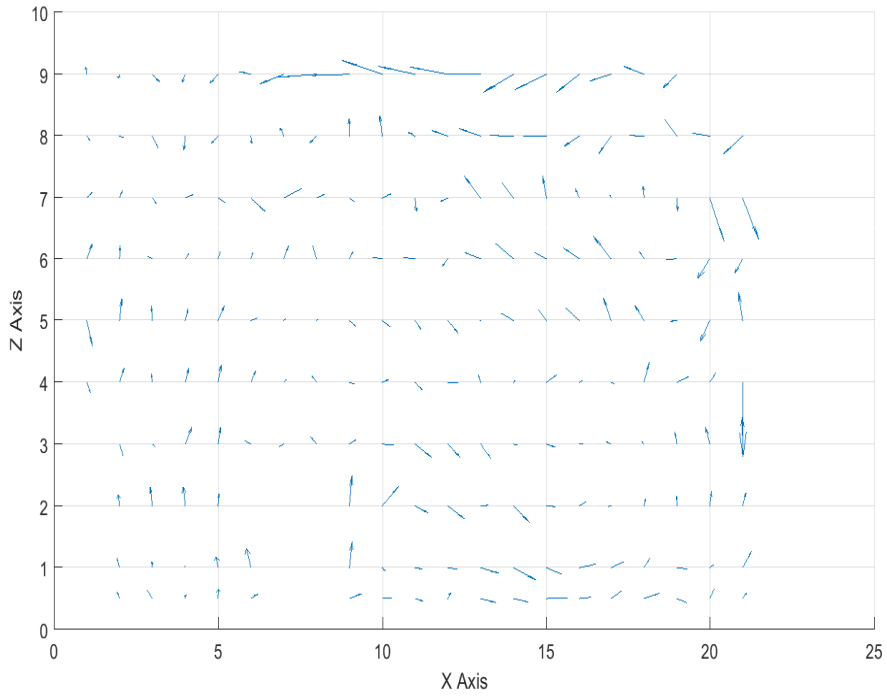

Figure 3.8: Two-dimensional resultants of air velocity in the XZ plane over the patient bed at y=3

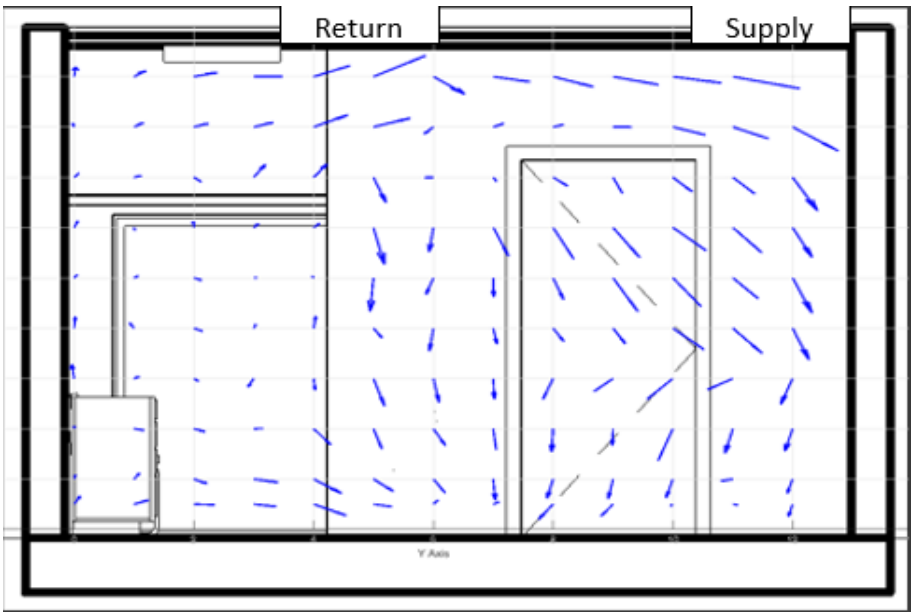

Figure 3.7: Approximate representation of two-dimensional resultants of air velocity in the YZ plane at x=13

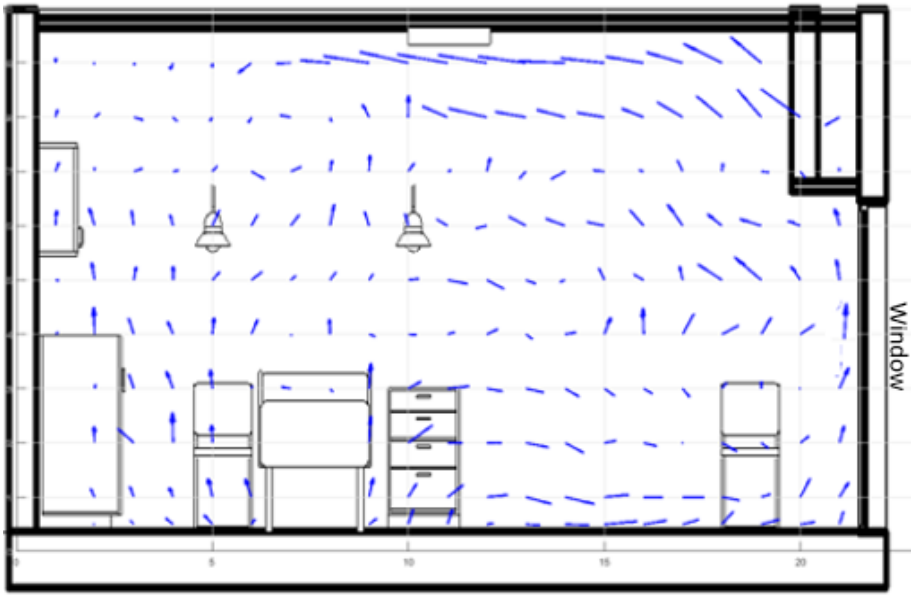

Figure 3.9: Approximate representation of two-dimensional resultants of air velocity in the XZ plane over the patient bed at y=3

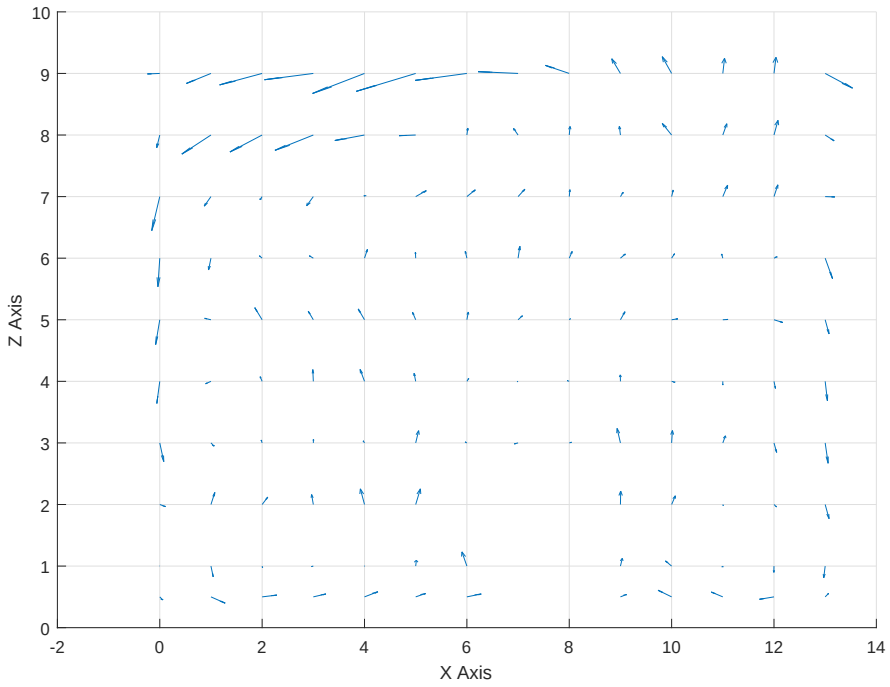

Figure 3.10: Two-dimensional resultants of air velocity in the XZ plane near return diffuser at y=6

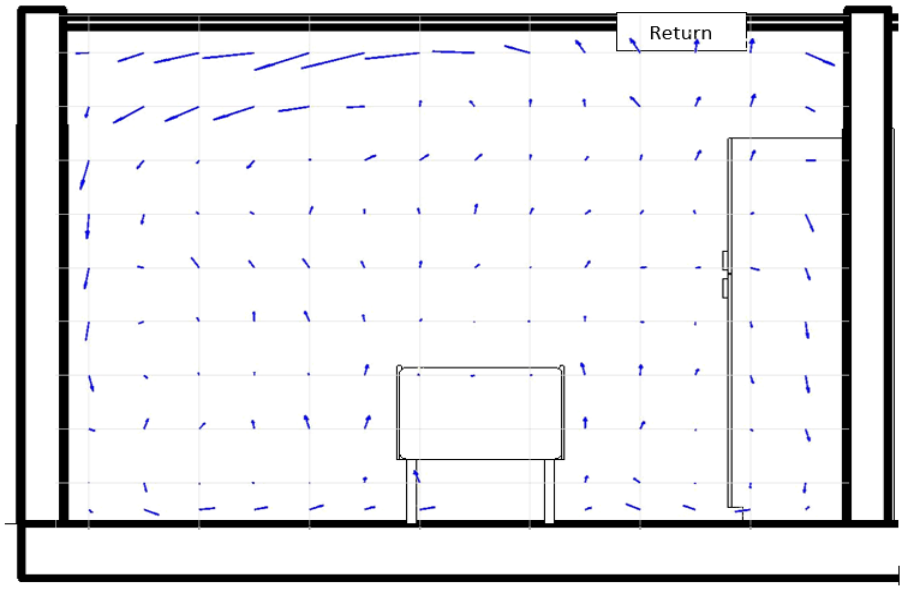

Figure 3.11: Approximate representation of two-dimensional resultants of air velocity in the XZ plane over the patient bed at y=6

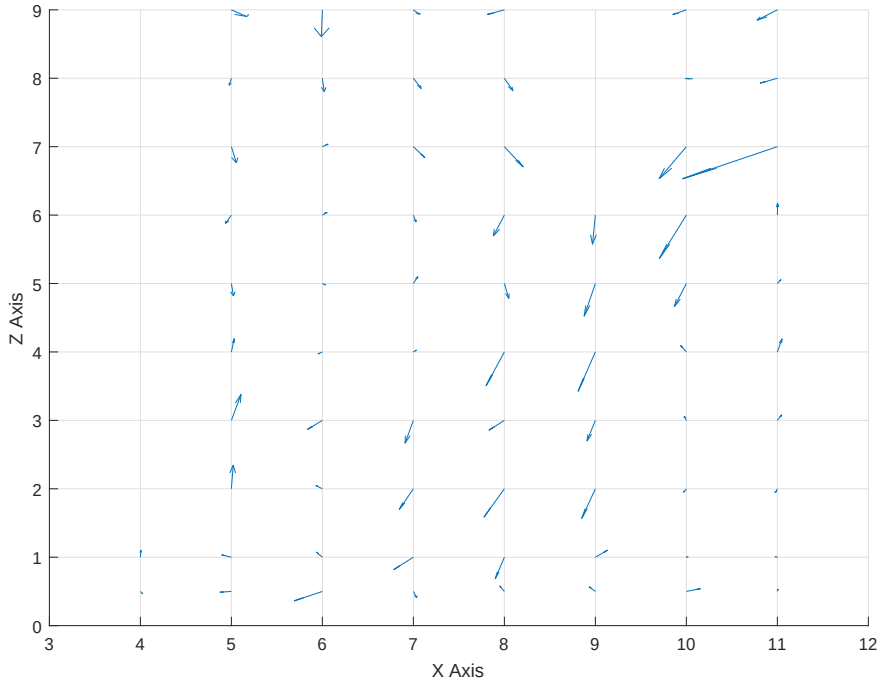

Figure 3.12: Two-dimensional resultants of air velocity in the XZ plane near supply diffuser at y=13

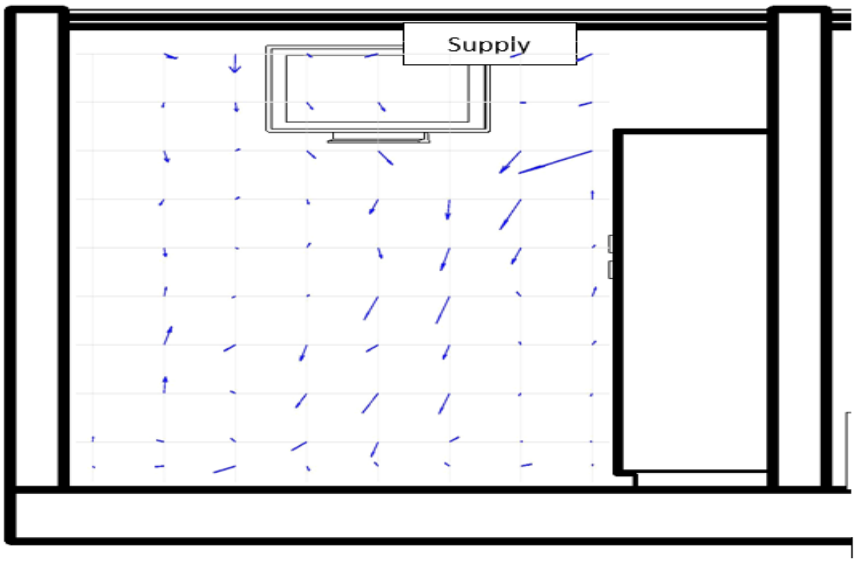

Figure 3.13: Approximate representation of two-dimensional resultants of air velocity in the XZ plane over the patient bed at y=13

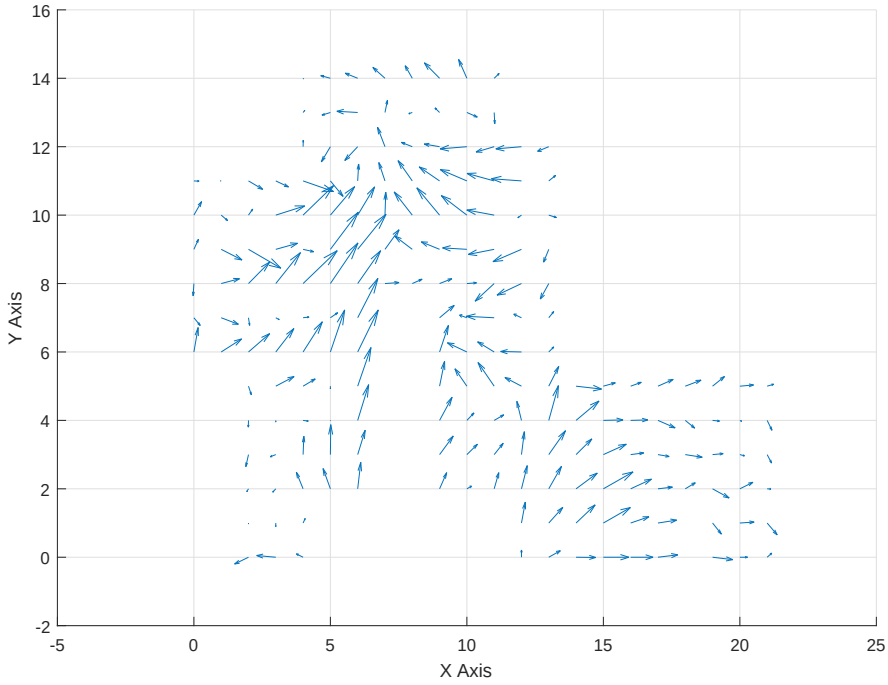

Figure 3.14: Two-dimensional resultants of air velocity in the XY plane 0.15m (0.5ft) above the ground

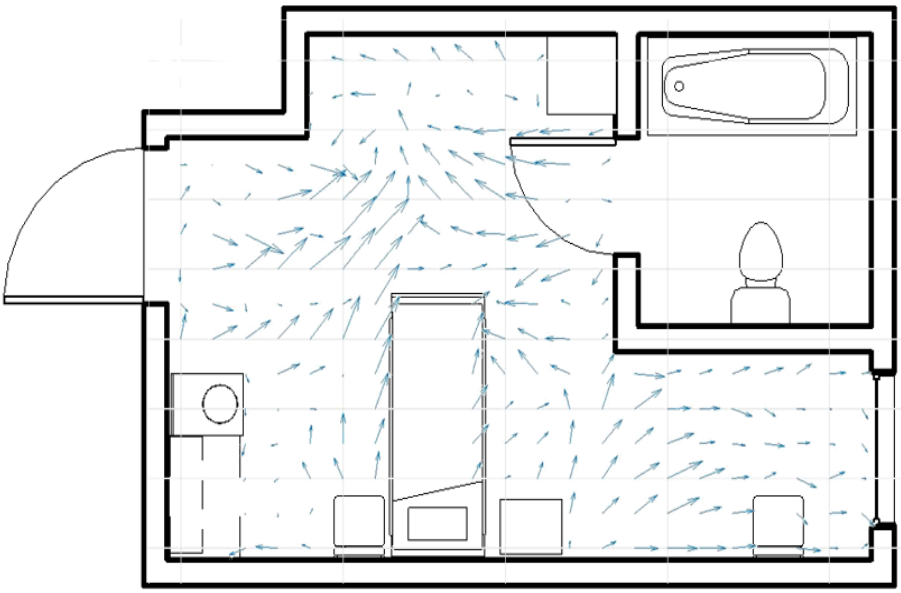

Figure 3.15: Approximate representation of two-dimensional resultants of air velocity in the XY plane 0.15m (0.5ft) above the ground

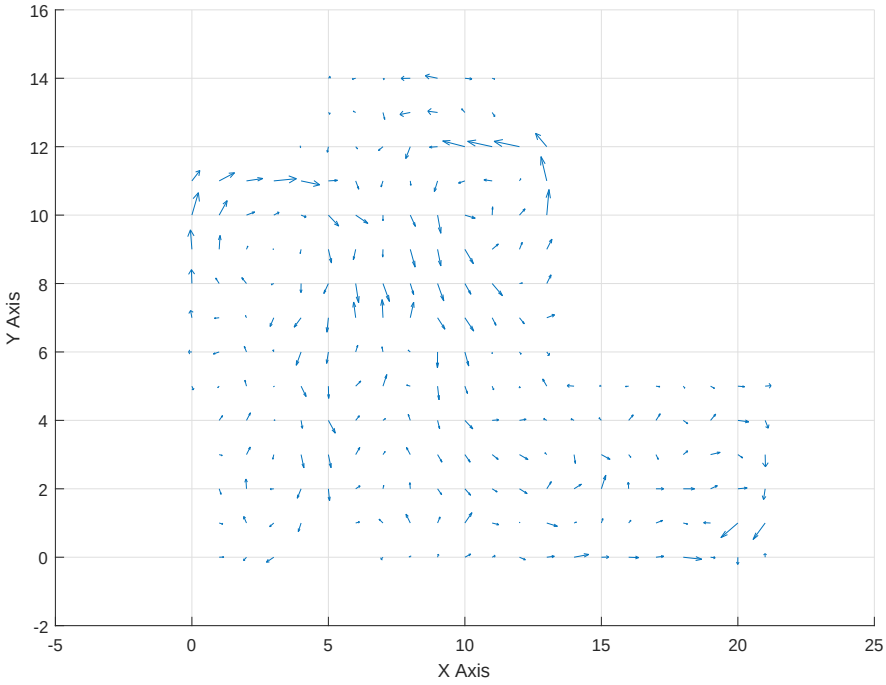

Figure 3.16: Two-dimensional resultants of air velocity in the XY plane 1.22m (4ft) above the ground

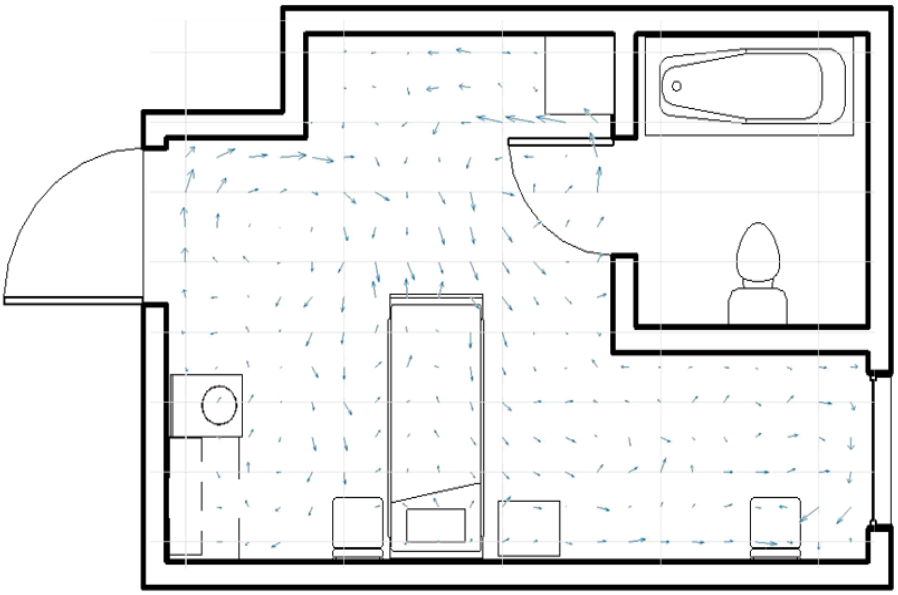

Figure 3.17: Approximate representation of two-dimensional resultants of air velocity in the XY plane 1.22m (4ft) above the ground

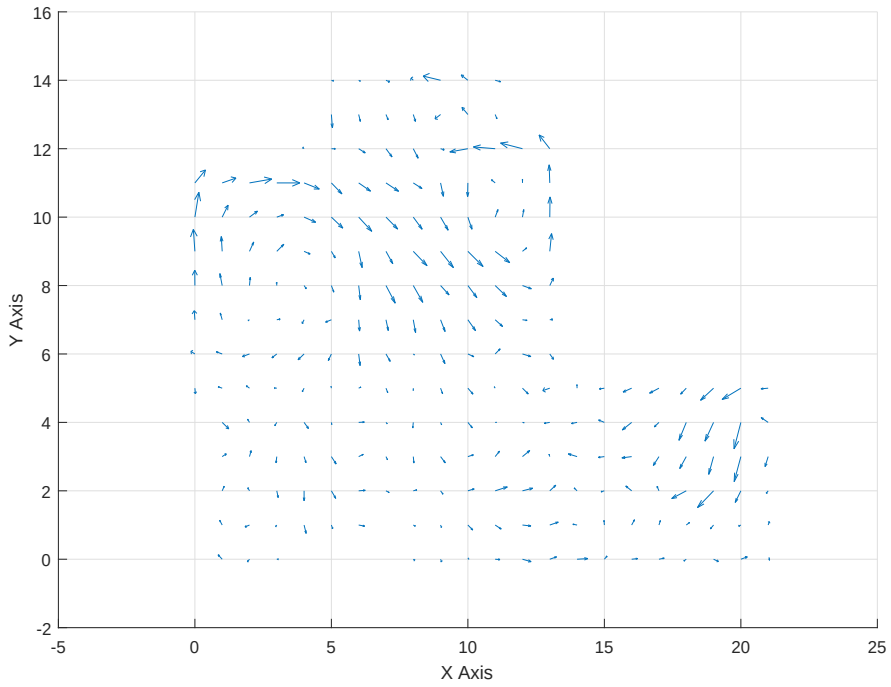

Figure 3.18: Two-dimensional resultants of air velocity in the XY plane 1.5m (5ft) above the ground

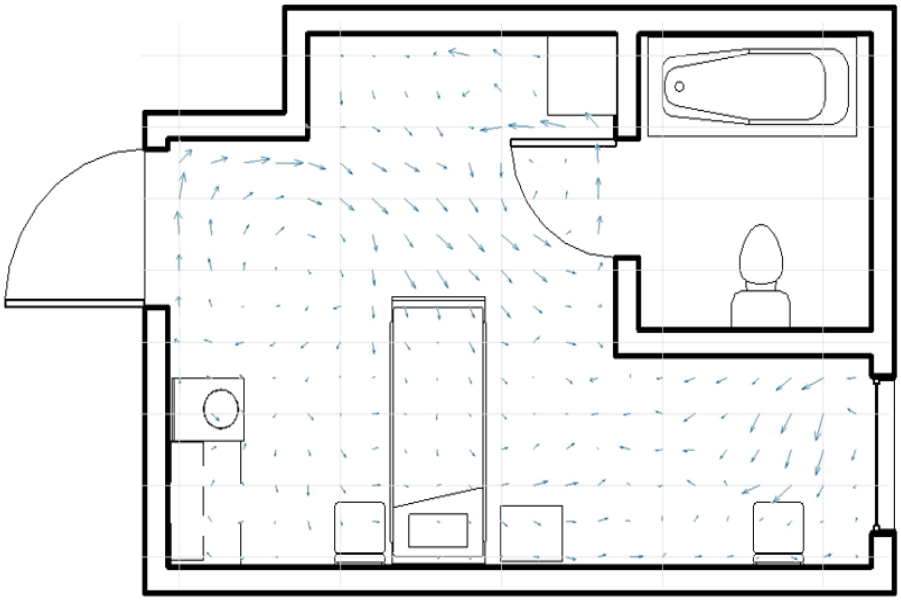

Figure 3.19: Approximate representation of two-dimensional resultants of air velocity in the XY plane 1.5m (5ft) above the ground

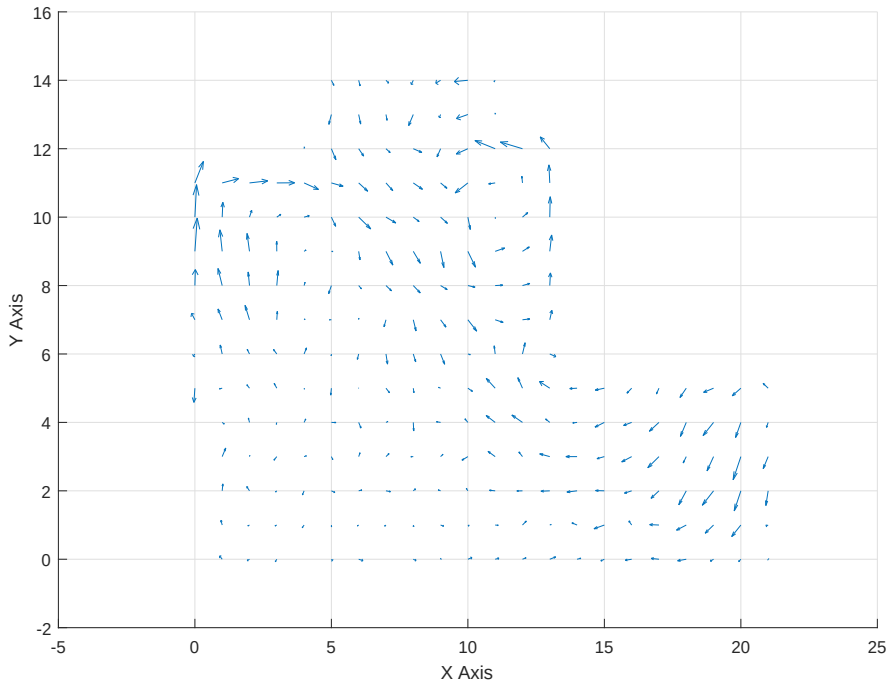

Figure 3.20: Two-dimensional resultants of air velocity in the XY plane 1.83m (6ft) above the ground

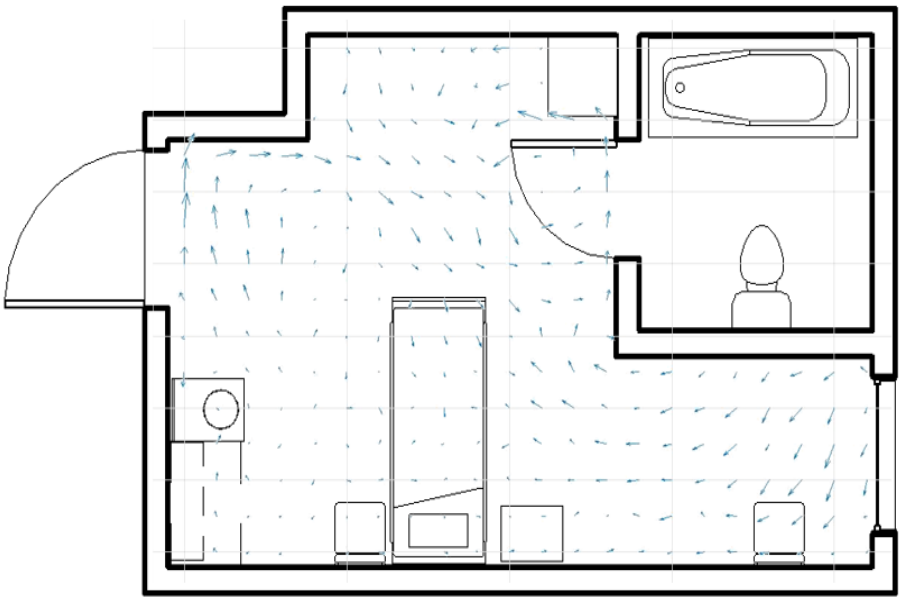

Figure 3.21: Approximate representation of two-dimensional resultants of air velocity in the XY plane 1.83m (6ft) above the ground

Figures 3.4 and figure 3.8 show velocity vectors over the patient bed. Upward air movement above patient bed, and downward air movement next to the wall seen in Figure 3.4, are due to natural convection. Air follows the circular path. Figure 3.6, figure 3.10 and figure 3.12 shows perpendicular sections that passes through the inlet and the outlet. Velocity is greater at the inlet and outlet. Air flow is downwards near the supply is because the supply air was cold. Figure 3.14 shows more turbulence in the airflow pattern and high velocities compare to airflow pattern and air velocities in figure 3.16 due to the furniture and other objects in the room. Airflow velocities were higher and more turbulent at a distance of 0.15m to 0.9m from the ground. At 1.22m distance from the ground and above (Figure 3.16 to 3.21) air follows similar pattern.

3.2 Root Mean Square Velocity Fluctuation Levels

Satanard deviation is a very efficient parameter describing the degree of variation or dispersion in a flow field. It is calculated as the square root of variance by determining the

variation between each data point relative to the mean. If the data points are further from the mean, there is higher deviation within the data set.

Mean Velocity:

$$\overline{V} = \int_{t}^{t+T} V(t)dt = 1/N \sum_{1}^{N} V_i \tag{3.2}$$

Standard Deviation:

$$s = \sqrt{\frac{\sum_{i=1}^{N} (V_i - \overline{V})^2}{(N-1)}} X100 \tag{3.3}$$

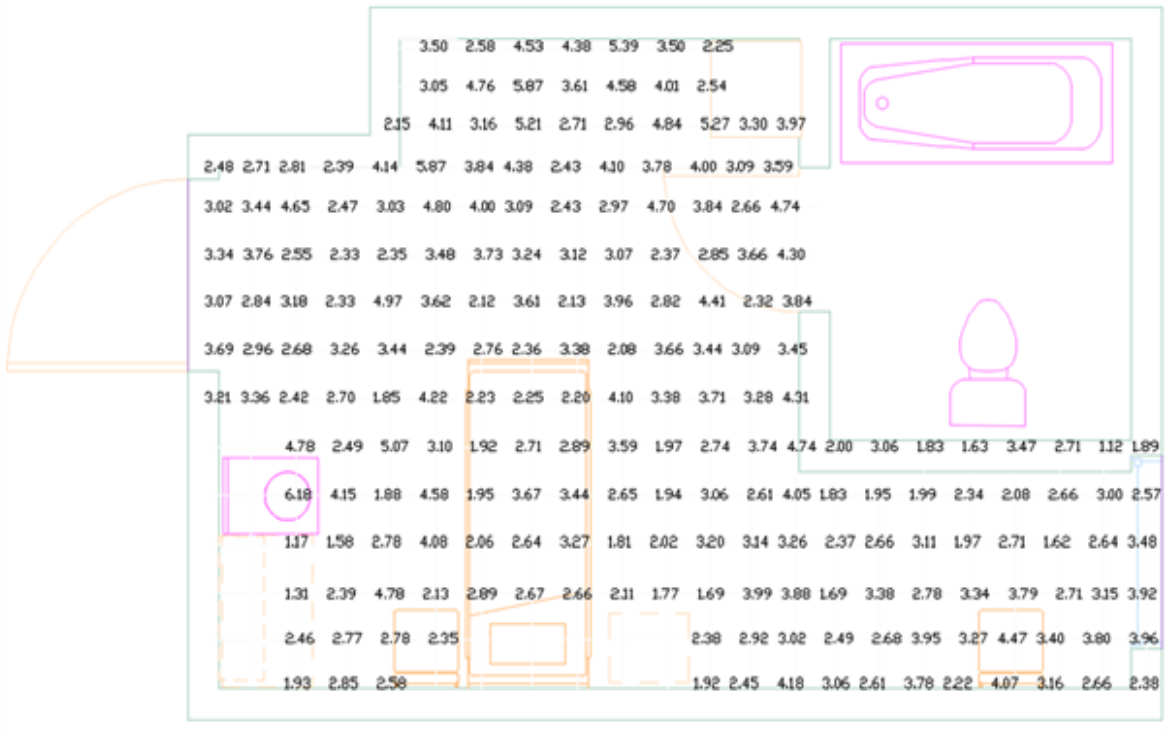

Figure 3.22: Standard Deviation in XY plane at 3ft above the ground

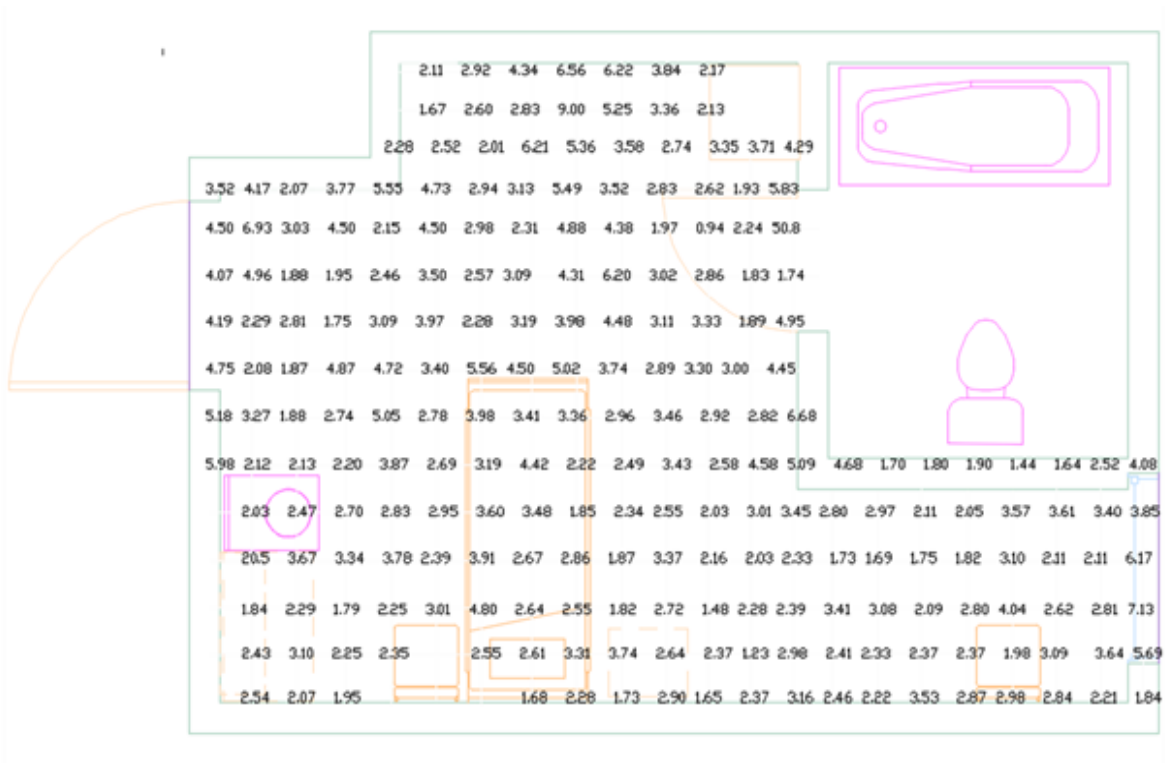

Figure 3.23: Standard Deviationy in XY plane at 4ft above the ground

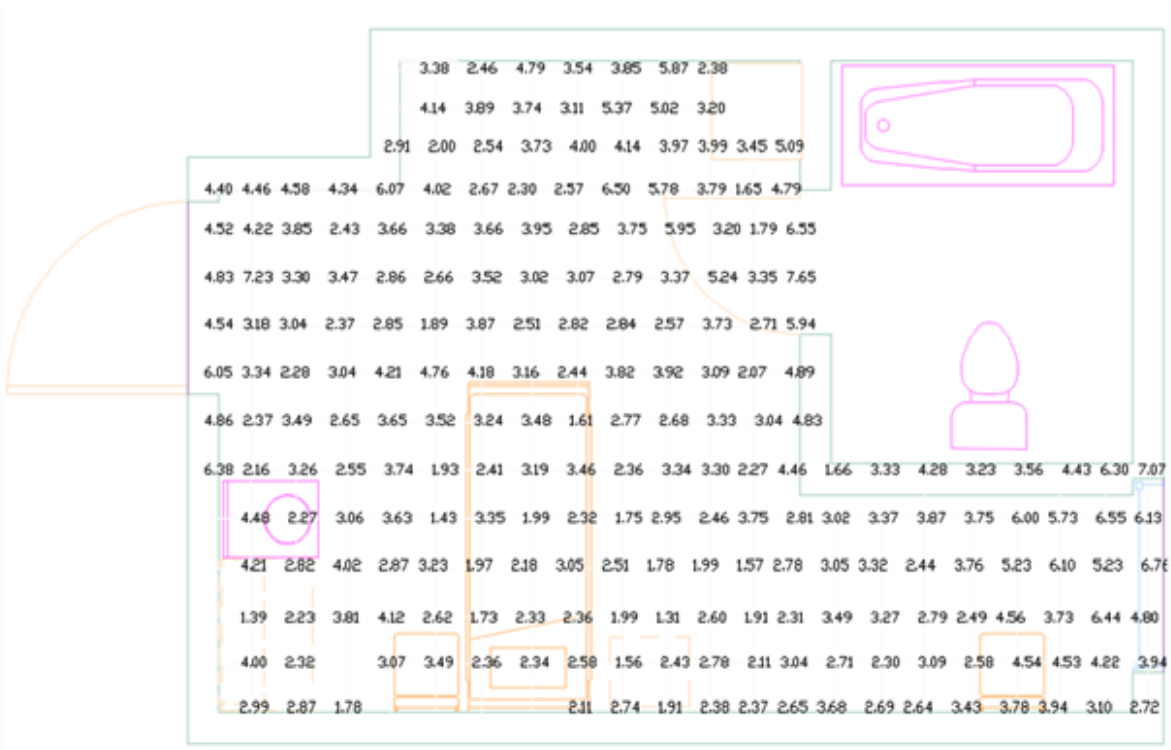

Figure 3.24: Standard Deviation in XY plane at 5ft above the ground

The standard deviation values were calculated at each grid point in the patient room. The forced ventilation, room geometry, and furnishings are expected to be possible causes of highly turbulent flow patterns in the patient room. With the standard deviation plots (figures 3.22, 3.23 and 3.24), it can be seen that highest Root Mean Square velocity values were measured between 1.3 X 10^{-2} m/s to 1.45 X 10^{-2} m/s near ceiling at a distance of 2.84m from the ground and the lowest Root Mean Square velocity values were measured between 0.03 X 10^{-2} m/s to 0.045 X 10^{-2} m/s near the ground. For reference the mean supply air velocity was 0.25 m/s.

3.3 Velocity Time Series

Contaminant Transport in Human Wakes: From a fluid mechanics perspective, the human form can be considered as a bluff body. Although limb movement complicates things a little, a walking human is essentially a non-aerodynamic, fronted shape passing through a fluid. This means that like all other bluff bodies, once moving beyond a certain speed an unsteady wake is produced. This is shown by Settles (2006) [76] in Figure 3.25. Although the wake produced will depend on the shape of the body, it is characterized by a low-pressure region 'behind' the body (where the body is assumed to be traveling 'forward'), separated flow and, if moving fast enough, vortex shedding [77]. The shed vortices carry large (relative to the ambient) quantities of vorticity, causing spiraling motions within the wake, entraining the surrounding fluid and enhancing mixing [78]. Therefore, should a walking person pass through a contaminated region of air, their ensuing wake will mix this air adding to its dispersion.

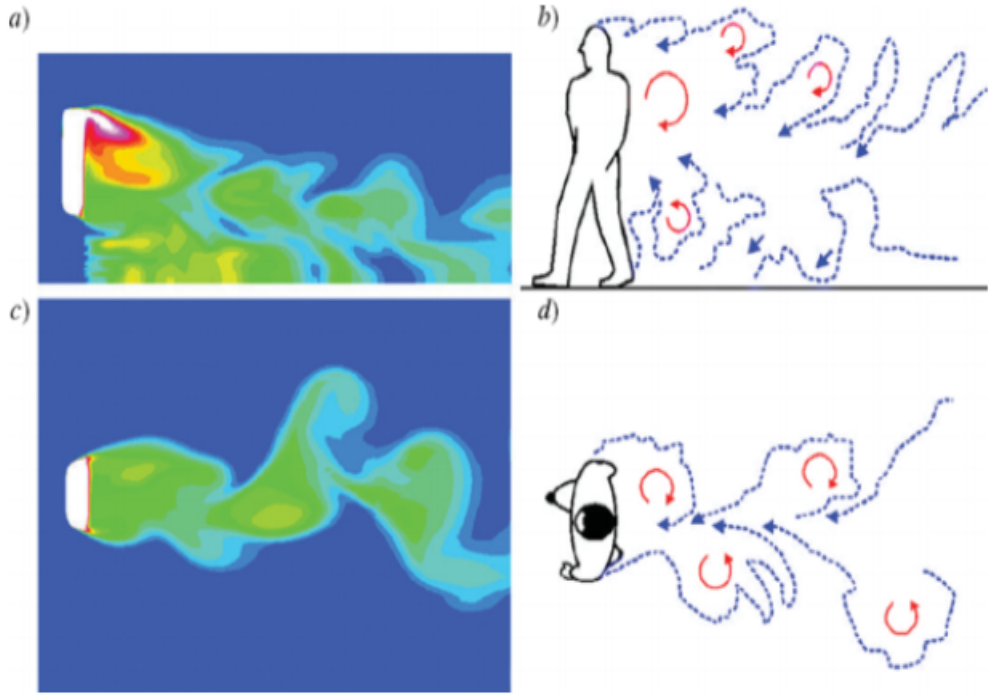

Figure 3.25: Images (b) and (d) show qualitative sketches of wake motions found during full-scale experiments, using smoke as a visualizing agent, while images (a) and (c) show the numerical counterparts. The wake entrainment processes are clearly visible in both approaches (Settles,2006).

A person with a forward projected area of 0.8 m^2 entering the patient room at 1m/s can further generate a 'body wake' of approximately 4 m^3 [65].

In order to analyze the turbulence profile vs. distance, air patterns near the patient were observed with a care provider walking around the patient bed at a distance of 0.3m (1ft), 0.6m (2ft), and 0.9m (3ft). The anemometer was placed over the bed near the patient's head at a distance at 1.2m above the ground. Figure 3.26 shows the location of the care provider near the patient bed. The patient was not lying in the bed when measurements were taken. During first and last 90 seconds there was no walking. Walking started after 90 seconds and continued until 31 seconds around the patient bed. The first 20 seconds of walking was a transition period, and we recorded measurements up to 90 seconds. The final 60 seconds of the sampling period was allotted to recording the decay in turbulence. For the first set of

this experiments, a care provider walked at a speed of 1.5 m/s around the sonic anemometer and 0.9m away from the patient bed. In the next two sets, the care provider walked in the predefined rectangular pattern at 0.6 and 0.3m distance from the bed, respectively. Figures 3.27 to 3.30 shows the walking patterns for all three sets of experiments. We used a timer to ensure consistency in walking speed.

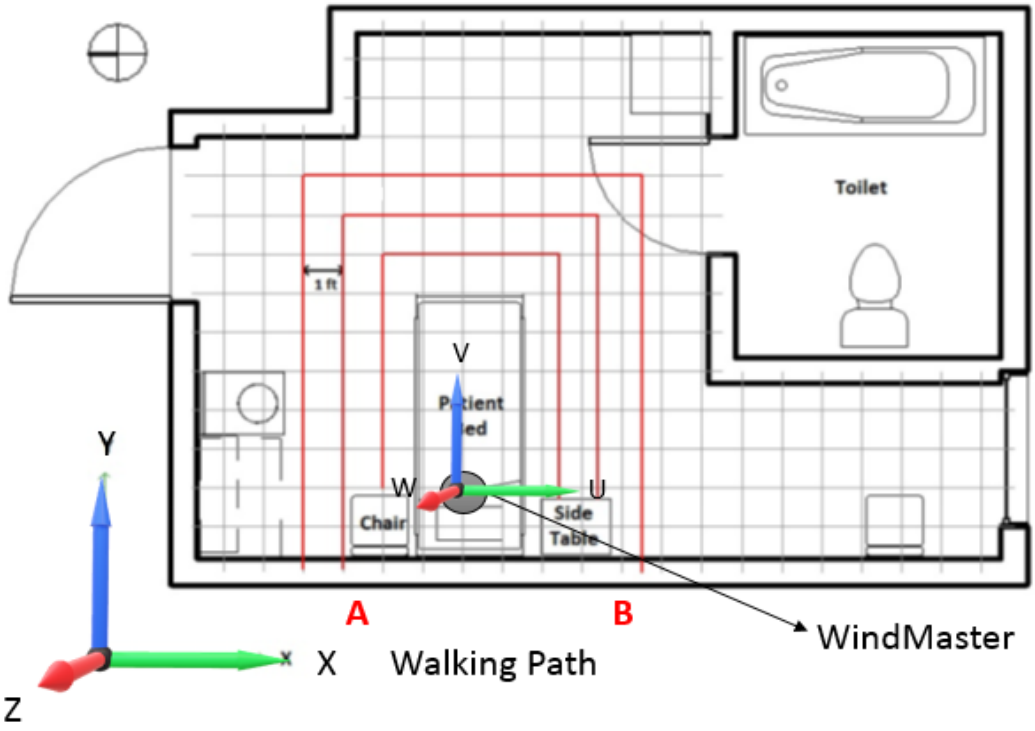

Figure 3.26: Walking patterns during measurement of velocity profiles with a sonic anemometer near the patient bed.

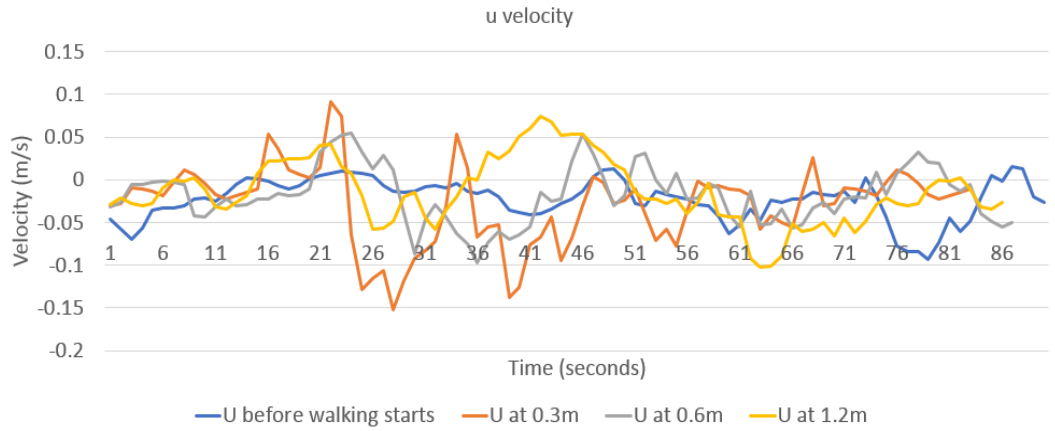

Figure 3.27: Time series of u direction velocity measured at the patient head walked around by one person, shown at varying distance from the patient bed.

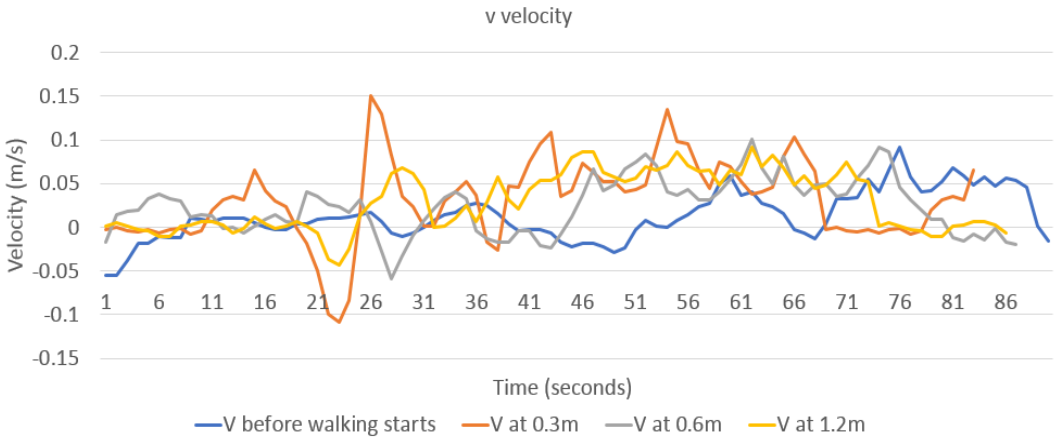

Figure 3.28: Time series of v direction velocity measured at the patient head walked around by one person, shown at varying distance from the patient bed.

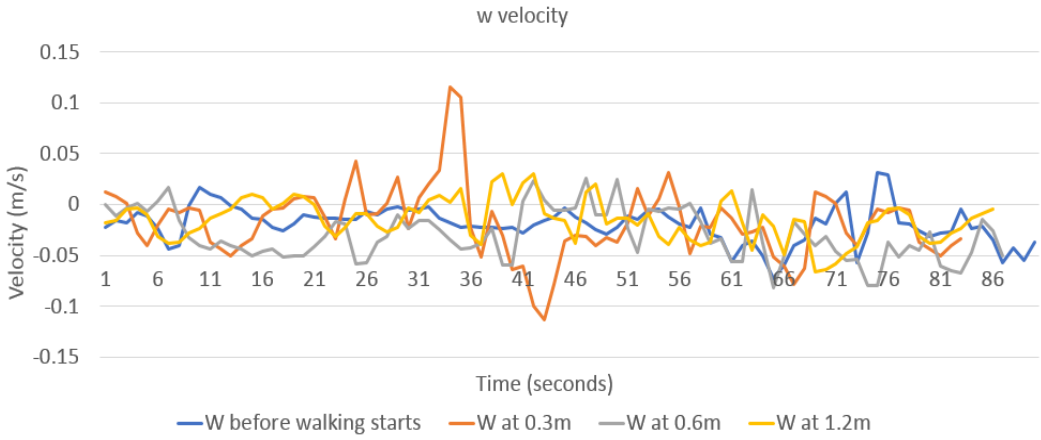

Figure 3.29: Time series of w direction velocity measured at the patient head walked around by one person, shown at varying distance from the patient bed.

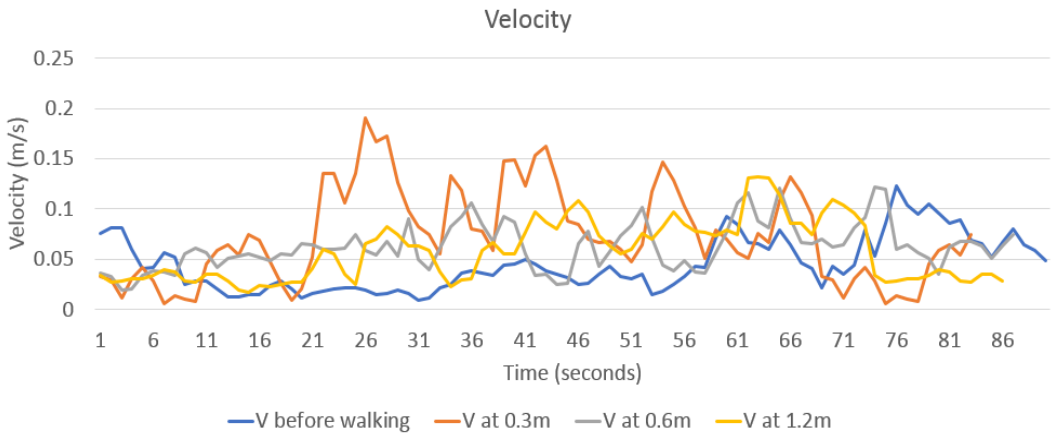

Figure 3.30: Time series of total velocity measured at the patient head walked around by one person, shown at varying distance from the patient bed.

The velocity fluctuations were largest at a distance of 0.3m from the patient bed and were lowest at a distance of 0.9m from the patient bed. The u component of the velocity showed more fluctuations when a care provider walked at 0.3m, 0.6m, and 0.9m from the bed. The fluctuations were greatest at 0.3m distance. The velocity fluctuations decayed after 51 seconds (Figure 3.27) and were similar to the background fluctuations (blue line in above 3.18 graph) in the room. The v component of the velocity showed more fluctuations when a care provider walked at 0.3m from the bed. The velocity fluctuations decayed after 70 seconds (Figure 3.28). Anemometer could not capture variations in v velocity because when

care giver walks in x direction the distance between anemometer and a care giver is large. The w component of the velocity showed more fluctuations when a care giver walked at 0.3m from the bed. The velocity fluctuations decayed after 45 seconds (Figure 3.30). Negative velocity values shows the change in the direction of a wind. Positive u velocity shows the direction of the wind towards the patient bed in X axis and the negative u velocity shows direction of wind towards the window. Similarly, v velocity is measured in Y direction and w velocity is measured in Z direction. Total velocity graph shows more fluctuations in velocities at 0.3m distance from bed. These results show that when a care giver walks at 0.3m distance from bed or 0.6m distance from anemometer, air above the patient head gets disturbed.

CHAPTER 4

Discussion

Most studies on the transmission of infectious disease particles have concentrated primarily on air changes per hour (ACH) and how ACH provides a dilution factor for possible infectious agents. Although increasing ventilation airflow rate does dilute concentrations better when the contaminant source is constant, it does not increase ventilation effectiveness. But the actual field experiment study by Mosavi [11] showed that, particles <1.0 μm exhibit different aerodynamic behaviors when compared to particles >1.0 μm in different environmental conditions. Higher ventilation rates have not been found to be proportionately effective in reducing aerosol concentrations. Specifically, increasing mechanical ventilation from 2.5 to 5.5 ACH reduced aerosol concentrations only 30% on average. However, particle concentrations were more than 40% higher in pathways between the source and exhaust as was the suspension and migration of larger particles ($3 - 10$ μm) throughout the patient room(s) [11]. These observations, however, ignore the spatial and temporal differences in rooms and assume a steady-state, well-mixed condition where ventilation rate, particle generation rate, and particle concentration in the supply are the same.

Memarzadeh's study [22] using CFD simulation suggests that in an enclosed and mechanically ventilated room (e.g., an isolation room), the dominant factor that affects the transmission and control of contaminants is the path between the contaminant source and exhaust. Contaminants are better controlled when this path is uninterrupted by an air stream. This observation of the impact of ventilation flow rate and infection risk is consistent with recent experimental studies [38, 68], which also found increasing airflow rates to 12ACH does not necessarily reduce the infection risk in a mixing ventilation setting. Other studies indicate that the interaction of coughed flow with high initial velocity with the free convection flow around the human body and the ventilation flow will be different than the flow of exhalation with much lower initial velocity [69] suggesting that the strategy of supplying extra amounts of outdoor air aiming to dilute the polluted room air may not be effective

in protecting from airborne cross-infection due to coughing.

If we compare the results from Mousavi's [11] and Memarzadeh's [22] study discussed above with the results obtained in this experiment, since the average wind speed above the patient bed was 0.068 m/s, larger particles will have a tendency to settle on the ground because of gravitational force and smaller particles ($<$1.0 μm) may get exhausted or remain suspended in this region. The results of this study also suggest that the most important contributing factor to contaminant transmission in enclosed and mechanically ventilated environments is the path between the contaminant source and the exhaust. In our experiment setup, exhaled air from the patient directly goes into the return diffuser. If this path is interrupted by air streams or other obstructions (e.g. a person walking) the contaminant is more likely to migrate to other places in the room. If this path is kept intact from an intercepting air stream, then the contaminant is unlikely to migrate.

CHAPTER 5

Conclusion

The results using sonic anemometry in the patient room demonstrated the benefits of using advanced instrumentation for direct air velocity measurements indoors. The application of CFD in any area of interest requires advanced knowledge and experience with both CFD and the phenomenon under investigation. When modeling buildings in CFD the spaces may need to be simplified which may not account for airflow changes due to furniture or other objects in the room. Results obtained in this study shows more turbulence in the airflow near furniture, supply and return diffusers. It is also difficult to model moving people in CFD simulations. Computational fluid dynamics simulations relies upon physical models of real-world processes. As with physical models, the accuracy of the CFD solution is only as good as the initial/boundary conditions provided to the numerical model. Also, because validation of CFD model predictions is always an issue, the availability of reliable, low-velocity ow data for direct comparison of modeling results can provide a higher level of confidence in the quality of simulated predictions. One goal of this study was to provide tools for better understanding air movement indoors and transport of toxic aerosols and bio-contaminants and consequently enhance the capabilities of real-time air monitors for occupants protection.

This study also shows that the effects of moving obstructions are easily recognizable in air speed continuous time series data. Moreover, the high sampling frequencies now available may provide high-resolution data on indoor turbulence. These data will prove helpful in understanding the movement and dispersion of indoor air pollutants. The sonic anemometer provides for direct measurements of air-velocity vector components and their fluctuations, which is valuable information. The benefit of using a sonic anemometer over tracer gas or smoke pens is that it provides velocities as well as direction which can be useful in determining thermal comfort and contaminant dispersion.

Result obtained in this experiment shows that the air above the patient bed goes directly into the return air diffuser located in the ceiling and its average wind speed is 0.068m/s. We

can determine the behavior of particles exhaled by the patient using Strokes law.

$$V_t = \frac{\rho_p d^2 g}{18\eta} C_c \tag{5.1}$$

$$C_c = 1 + \frac{2\lambda}{d}(A_1 + A_2 e^{-\frac{A_3 d}{\lambda}}) \tag{5.2}$$

where ρ_p is the density of the particle (kg/m^3) (assumed as 1000 kg/m^3), d is the particle diameter (m), g is the acceleration due to gravity (9.81 m/s^2), h is the viscosity of air (1.78 X $10^{-}5$ kg/ms), and C_c is the Cunningham slip-correction factor, λ is the mean free path, d is the particle diameter and A_1,A_2 and A_3 are experimentally determined coefficients. For air (Davies, 1945) $A_1 = 1.257$, $A_2 = 0.400$, $A_3 = 0.55$.

Particle Diameter (μm)	**Terminal Velocity (m/s)**	**Time required to fall 2m (min)**	**Time required to fall 1.22m (min)**
0.1	9.96162E-07	33461.8	20411.67
0.2	2.60468E-06	12797.5	7806.45
0.3	4.82556E-06	6907.7	4213.67
0.5	1.11044E-05	3001.8	1831.11
1	3.75178E-05	888.5	541.96
5	0.00080	41.7	25.42
10	0.00313	10.6	6.49
15	0.00699	4.8	2.91
20	0.01239	2.7	1.64
25	0.01931	1.73	1.05
30	0.02776	1.20	0.73
35	0.03775	0.88	0.54
40	0.04926	0.68	0.41
45	0.06231	0.53	0.33
50	0.07689	0.43	0.26
55	0.09300	0.36	0.22
60	0.11064	0.30	0.18

Table 5.1: Terminal velocity of falling particles

Table 5.1 shows the terminal velocity of particles falling through air and duration of

fall calculated using Stoke's law. Small changes in diameter can greatly influence terminal velocity. Looking at the airflow patterns in this experiment and data from above table (Table 5.1) we can make the general statement about the particles liberated from a patient that particles greater than 50 μm in diameter might remain suspended in the air and settle on the ground due to gravitational force and particles less than 50 μm in diameter are likely to be extracted since their terminal velocity is far less than average air velocity above the patient bed and the airflow pattern above the patient bed and exhaust is uninterrupted.

The limitation of this study included the difficulty in capturing airflows in congested spaces. The diameter of this instrument is 240mm, so it could not capture air velocities between gaps less than 240mm. An additional limitation was measurement is time intensive. It took 3 weeks to measure airflows in the patient room. Additionally, weather and time of the day must be considered. Outside weather, indoor conditions and time of measurements should be approximately the same for every experiment so that the boundary conditions will be same during the experiment.

CHAPTER 6

Future Work

Natural ventilation is another option for infection control because it can provide high ventilation rates and is energy efficient. A World Health Organization (WHO 2009) report on the use of natural ventilation notes that where droplet nuclei are an important mode of disease transmission, average quanta production rates in subjects are usually <1 quanta/minute. With a quanta production rate of 10 quanta/minute, the estimated risk of infection with 15 minutes of exposure in a room with 12 ACH is 4 percent, and with 24 ACH it is 2 percent. This illustrates the importance of adequate ventilation [56]. A major advantage of natural ventilation in healthcare facilities is the significant ventilation rates (18-24 ACH) that can be achieved for wards which can be a bonus if airborne infection is a risk [46]. In their study of a Hong Kong hospital, Qian et al. [46] showed that up to 69 ACH was possible given the right environmental conditions and that when carefully integrated with exhaust fans, such hybrid systems can eliminate the unreliability of driving forces like wind or problems associated with pressure breakdown due to activities like the opening of doors [49]. The World Health Organization (WHO) has documented a specific guideline for natural ventilation of hospitals, in which it strongly recommends the rate of 60 l/s/patient [47]. However, there is no specific guidance on how this rate can be accomplished with acceptable climatic conditions or for that matter, what the rates should be during winter when trickle ventilation needs to be maintained [48]. The use of an anemometer can measure, airflow rate in naturally ventilated spaces similarly to the method used in this experiment. The results obtained from analysis of naturally ventilated spaces can be compared to mechanically ventilated spaces to understand airflow patterns and energy savings. Airflow rates, direction and temperature between the different ventilation strategies can be compared.

Also for mechanical ventilation different supply and exhaust locations can be compared to study the air flow path between patient and exhaust to analyze infection risk. Begg's [27]

performed Computational Fluid Dynamics simulations for three different locations of supply and exhaust diffusers in a 32 m^3 patient room using Fluent 6.2 CFD software. In all three cases, the total air ow rate was set to be equivalent to 6 air change per hour, and a zero pressure condition was defined on the extract diffuser boundary. The lowest average value of bio-aerosol concentration was seen in the condition where the supply and exhaust are located in the ceiling. Khankari [75] also performed a similar study in a 51.78 m^3 patient room using computational fluid dynamics simulation. His study indicates that placement of return grille right behind the linear supply diffuser over patient's head is effective for infection control. We can test these conditions using a sonic anemometery to verify their findings.

References

[1] Coronado VG, Beck-Sague CM, Hutton MD, et al. Transmission of multidrug-resistant Mycobacterium tuberculosis among persons with human immunodeficiency virus infection in an urban hospital: epidemiologic and restriction fragment length polymorphism analysis, J. Infect. Dis. **168(4):1052-5** (1993)

[2] Bloch AB, Orenstein WA, Ewing WM, et al. Measles outbreak in a pediatric practice: airborne transmission in an office setting. Pediatrics. **75(4):676-83** (1985)

[3] LeClair JM, Zaia JA, Levin MJ, Congdon RG, Goldmann DA. Airborne transmission of chickenpox in a hospital. N. Engl. J. Med. **302(8):4503** (1980)

[4] Riley RL, Mills CC, Nyka W, et al. Aerial dissemination of pulmonary tuberculosis. A two-year study of contagion in a tuberculosis ward. 1959. Am. J. Hyg. **70:185-96** (1959)

[5] CDC. Guidelines for Environmental Infection Control in Health-Care Facilities. Recommendations of CDC and the Healthcare Infection Control Practices Advisory Committee (HICPAC). MMWR. **52(RR10)** (2003) 1-42

[6] CDC. Guidelines for preventing the transmission of Mycobacterium tuberculosis in health-care settings, 2005. MMWR Recomm. Rep. **54(17)** (2005) 1-141

[7] Beck-Sague C, Dooley SW, Hutton MD, et al. Hospital outbreak of multidrug-resistant Mycobacterium tuberculosis infections. Factors in transmission to staff and HIV-infected patients. JAMA.**268(10)12806** (1992).

[8] CDC. Guidelines for preventing the transmission of Mycobacterium tuberculosis in health-care facilities, 1994. Centers for Disease Control and Prevention. MMWR Recomm. Rep.**43(RR-13):1-132** (1994)

[9] Haley CE, McDonald RC, Rossi L, Jones WD, Jr., Haley RW, Luby JP. Tuberculosis epidemic among hospital personnel. Infect. Control Hosp. Epidemiol.**10(5):204-10** (1989)

[10] Cole EC, Cook CE. Characterization of infectious aerosols in health care facilities: an aid to effective engineering controls and preventive strategies. Am. J. Infect. Control. **26(4):453-64** (1998).

[11] Ehsan S. Mousavi, Kevin R. Grosskopf, Ventilation Rates and Airflow Pathways in Patient Rooms: A Case Study of Bioaerosol Containment and Removal,, Ann Occup Hyg **59 (9): 1190-1199**, (2015)

[12] Grosskopf KR Mousavi ES., Ventilation and transport bioaerosols in health-care environments. ASHRAE Journal, **56: 22-31** (2014).

[13] Kowalski WJ, Air-treatment systems for controlling hospital-acquired infections. HPAC Eng., **79: 28-48** (2007).

[14] AIA, Guidelines for Design and Construction of Health Care Facilities . Second edition, Washington, DC: The American Institute of Architects.(2006)

[15] Siegel JD Rhinehart E Jackson M et al, 2007 guideline for isolation precautions : preventing transmission of infectious agents in healthcare settings Am J Infect Control. **35: S65-S124** (2007)

[16] ASHRAE. (2008) Standard, 170-2008 Ventilation of Health Care Facilities . Atlanta, GA: ASHRAE.

[17] Atkinson J Chartier Y Pessoa-Silva CL et al, Natural ventilation for infection control in health-care settings , World Health Organization. ISBN 978 92 4 154785 7 (2009)

[18] Marshall JW Vincent JH Kuehn TH et al Studies of ventilation efficiency in a protective isolation room by the use of a scale model. Infect Control. **17: 5-10** (1996)

[19] Novoselac A Srebric J., Comparison of air exchange efficiency and contaminant removal effectiveness as IAQ indices. ASHRAE Trans ; **109: 339-49** (2003)

[20] Walker JT Hoffman P Bennett AM et al . Hospital and community acquired infection and the built environment - design and testing of infection control rooms. J Hosp Infect. **65: 43-9** (2007)

[21] Johnson DL Lynch RA Mead KR.,Containment effectiveness of expedient patient isolation units. Am J Infect Control. **37: 94-100**(2009)

[22] Memarzadeh F Xu W., Role of air changes per hour (ACH) in possible transmission of airborne infections. Build Simulation ; bf 5: 15-28 (2011)

[23] Hyttinen M Rautio A Pasanen P et al., Airborne infection isolation rooms - A review of experimental studies. Indoor Built Environment **20: 584-94**(2011)

[24] Rydock JP Eian PK., Containment testing of isolation rooms. J Hosp Infect. **57: 228-32** (2004).

[25] Kowalski WJ., Air-treatment systems for controlling hospital-acquired infections. HPAC Engineering, **79: 28-48** (2007)

[26] ASHRAE/ASHE Standard, 170-2008. Ventilation of Health Care Facilities. Atlanta: American Society of Heating, Refrigerating and Air-conditioning Engineers. (2008)

[27] Beggs CB, Kerr KG, Noakes CJ, Hathway EA, Sleigh PA., The ventilation of multiple-bed hospital wards: Review and analysis. American Journal of Infection Control, **36: 250-259** (2008)

[28] Duguid JP., The size and the duration of air-carriage of respiratory droplets and expelled from the human respiratory tract during expiratory activities. Journal of Aerosol Science, **40: 256-269** (1945)

[29] Fairchild CI, Stamper JK., Particle concentration in exhaled breath. American Industrial Hygiene Association Journal, **48: 948-949** (1987)

[30] Fennelly KP, Martyny JW, Fulton KE, Orme IM, Cave DM, Heifets LB., Cough-generated aerosols of Mycobacterium tuberculosis: A new method to study infectiousness. American Journal of Respiratory and Critical Care Medicine, **169: 604-609** (2004).

[31] Papineni RS, Rosenthal FS., The size distribution of droplets in the exhaled breath of healthy human subjects. Journal of Aerosol Medicine, **10: 105-116** (1997)

[32] Morawska L, Johnson GR, Ristovski ZD, Hargreaves M, Mengersen K, Corbett S, Chao, CYH, Li Y, Katoshevski D., Size distribution and sites of origin of droplets expelled from the human respiratory tract during expiratory activities. Journal of Aerosol Medicine, **40: 256-269** (2009)

[33] Hoppe P., Temperature of expired air under varying climatic conditions. International Journal of Biometeor, **25: 127-132** (1981)

[34] Zhu S, Kato S, Yang JH., Investigation into airborne transport characteristics of airflow due to coughing in a stagnant room environment. ASHRAE Transactions, **112(1): 123-133** (2006).

[35] Wells WF., Airborne Contagion and Air Hygiene: An Ecological Study of Droplet Infections. Cambridge, USA: Harvard University Press. (1955)

[36] Cole EC, Cook CE., Characterization of infectious aerosols in health care facilities: an aid to effective engineering control and preventive strategies. American Journal of Infection Control, **26: 453-464** (1998).

[37] Fitzgerald D, Hass DW. Mycobacterium tuberculosis. In: Mandell GL, Bennett, JE, Dolin R (eds), Principles and Practice of Infectious Diseases, 6th edn. Philadelphia: Churchill Livingston, pp. 2852-2886 (2005)

[38] Kierat W, Bolashikov ZD, Melikov AK, Popiolek Z, Brand M., Exposure to coughed airborne pathogens in a double bed hospital patient room with overhead mixing ventilation: Impact of posture of coughing patient and location of doctor. In: Proceedings of ASHRAE IAQ 2010.

[39] Bolashikov ZD, Kierat W, Melikov AK, Popiolek Z., Exposure of health care workers to coughed airborne pathogens in a hospital room with overhead mixing ventilation: Impact of the ventilation rate and the distance downstream from the coughing patient. In: Proceedings of IAQ 2010, Airborne Infection Control-Ventilation, IAQ and Energy, Kuala Lumpur, Malaysia. (2010)

[40] Cheong KWD, Phua SY., Development of ventilation design strategy for effective removal of pollutant in the isolation room of a hospital. Building and Environment, **41: 1161-1170** (2006).

[41] Noakes CJ, Fletcher LA, Sleigh PA, Booth WB, Beato-Arribas B, Tomlinson N., Comparison of tracer techniques for evaluating the behaviour of bioaerosols in hospital isolation rooms. In: Proceedings of Healthy Buildings 2009, Syracuse, USA. (2009)

[42] Tung YC, Shih YC, Hu SC., Numerical study on the dispersion of airborne contaminants from an isolation room in the case of door opening. Applied Thermal Engineering, **29: 1544-1551** (2009a)

[43] Tung YC, Hu SC, Tsai TI, Chang IL., An experimental study on ventilation efficiency of Isolation room. Building and Environment, **44: 271-279** (2009b)

[44] Menzies D., Hospital ventilation and risk for tuberculous infection in canadian health care workers. Ann Intern Med ; **133: 779**(2000)

[45] Steven J. Emmerich , David Heinzerling , Jung-il Choi, Andrew K. Persily, Multizone modeling of strategies to reduce the spread of airborne infectious agents in healthcare facilities. (2012)

[46] H. Qian, Y. Li, W.H. Seto, P. Ching, W.H. Ching, H.Q. Sun, Natural ventilation for reducing airborne infection in hospital, Building Environ, **45** (2010), 559-565.

[47] J. Atkinson, Y. Chartier, C.L. Pessoa-Silva, P. Jensen, Y. Li, W.-H. Seto (Eds.), Natural ventilation for infection control in health-care settings, WHO Guideline, p. WX167 (2009)

[48] Y. Li, M.K.H. Leung, W.H. Seto, P.L. Yeun, J. Leung, J.K. Kwan, et al., Factors affecting ventilation effectiveness in SARS wards, Hong Kong Med J, 14 (2008), pp. 33-36

[49] Z.A. Adamu, A.D.F. Price, M.J. Cook, Performance evaluation of natural ventilation strategies for hospital wards - A case study of Great Ormond Street Hospital (2012)

[50] Atkinson, J., Chartier, Y., and Pessoa-Silva, C. L. Nonserial Publication : Natural Ventilation for Infection Control in Health-care Settings. Albany, CH: World Health Organization. (2009)

[51] Paul Ninomura, J. B., New Ventilation Guidelines For Health-Care Facilities. (2001)

[52] Ross, C. d., Studies on fungal and bacterial population of air-conditioned environments. (2004)

[53] Heather Burpee, E. M., Comparative Analysis of Hospital Energy Use: Pacific Northwest and Scandinavian. (2013)

[54] Architecture 2030. The 2030 challenge. Retrieved from http://www.architecture2030.org/2030-challenge/index.html (2011)

[55] Energy Information Administration. Commercial buildings energy consumption survey (CBECS). Washington, DC: U.S. Department of Energy. (2007)

[56] Farhad Memarzadeh, PhD, PE, Literature Review: Room Ventilation and Airborne Disease Transmission., (2013)

[57] Hospital Ventilation and Tuberculosis in Canadian Health Care Workers. Ann Intern Med.;133:S-52. doi: 10.7326/0003-4819-133-10-200011210-00005 (2000)

[58] Faulkner, W. B., et al., Particulate Concentrations Within a Reduced-Scale Room Operated at Various Air Exchange Rates. (2013)

[59] Gold, E., and G. A. Nankervis., Cytomegalovirus. In Viral Infections of Humans, edited by A. Evans, **175-76** New York: Plenum Medical Book Co.(1989)

[60] Greene, V. W., Microbiological Contamination Control in Hospitals. Hospitals **43 (20)** (1969) 78-88.

[61] Yu, I. T. S., et al., Temporal-Spatial Analysis of Severe Acute Respiratory Syndrome Among Hospital Inpatients. Clinical Infectious Diseases **40 (9):12** (2005) 37-43.

[62] Gregory, P. H., Microbiology of the Atmosphere. Leonard Hill, Plymouth. (1973)

[63] Hyttinen, M., Rautio, A., Pasanen, P., Reponen, T., Earnest, G., Streifel, A., and Kalliokoski, P., Airborne Infection Isolation Rooms - A Review of Experimental Studies. Indoor and Built Environment **20(6), 584-594** (2011)

[64] Beggs, C., Donnelly, J., Kerr, K., Sleigh, P., Mara, D., and Cairns, G., The Use of Engineering Controls to Disinfect Mycobacterium tuberculosis and Airborne Pathogens in Hospital Buildings. Indoor+ Built Environment, **9(1), 17-27** (2000)

[65] Li, Leung, Tang, Yang, Chao, Lin, Yuen., Role of ventilation in airborne transmission of infectious agents in the built environment - a multidisciplinary systematic review. Indoor Air, **17(1)** (2007), 2-18.

[66] 1590-PK-020/W WindMaster user manual by Gill Instruments Limited, Saltmarsh Park, 67 Gosport Street, Lymington, Hampshire, SO41 9EG, UK.

[67] Airdata Multimeter ADM-880C user manual by Shortridge Instruments, Inc., 7855 East Redfield Road, Scottsdale, Arizona 85260.

[68] Nielsen PV, Olmedo I, Ruiz de Adana M, Grzelecki P, Jensen RL., Airborne cross infection between two people in a displacement ventilated room. HVAC and R Research. (in presss) (2011).

[69] Gupta JK, Lin CH, Chen Q., Characterizing exhaled airflow from breathing and talking. Indoor Air, **20: 31 - 39** (2010).

[70] Wells W. F., Airborne contagion and air hygiene. Cambridge, MA: Harvard University Press.(1955)

[71] Catherine J. Noakes and P. Andrew Sleigh, Mathematical models for assessing the role of airflow on the risk of airborne infection in hospital wards.(2009)

[72] Alireza Kermani 920150, CFD Modeling for Ventilation System of a Hospital Room, Excerpt from the Proceedings of the 2015 COMSOL Conference in Boston.(2015)

[73] Khodakarami, and Nasrollahi, Thermal comfort in hospitals - A literature review. Renewable and Sustainable Energy Reviews, **16(6), 4071-4077** (2012).

[74] R. Kameel, E. Khalil, Thermal comfort VS air quality in air-conditioned healthcare applications. 36th AIAA thermophysics conference 2003, Orland, Florida, paper no. AIAA-2003-40199 (2003)

[75] K. Khankari, Airflow path matters patient room HVAC. ASHRAE Journal June 2016

[76] Settles, G., Fluid Mechanics And Homeland Security. Annual Review Of Fluid Mechanics, **38:87-110** (2006).

[77] Poussou, S. B. and Plesniak, M. W., Vortex Dynamics And Scalar Transport In The Wake Of A Bluff Body Driven Through A Steady Recirculating Flow. Experiments In Fluids, **53(3):747-763** (2012).

[78] Cohen, L. S. and Director, M. N., Transport Processes In The Two-Dimensional Near Wake. The American Institute of Aeronautics and Astronautics Journal, **13(8):969-970** (1975).

[79] Granich R, Binkin NJ, Jarvis WR, Simone PM, Guidelines for the prevention of tuberculosis in health care facilities in resource-limited settings. WHO/CDS/TB99.269 ed. Geneva: World Health Organization., (1999)

[80] Ray Pradinuk, Incentivizing the Daylit Hospital: The Green Guide for Health Care Approach, Health Environments Research and Design Journal **1937-5867** (2009)

Appendix A: Two-dimensional resultants of air velocity in the XY plane

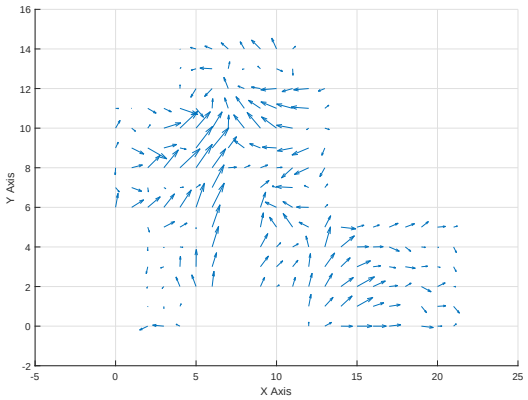

Figure 6.1: At Z=0.15 m

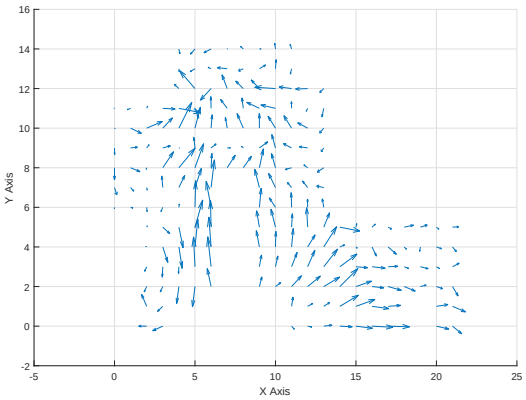

Figure 6.2: At Z=0.3 m

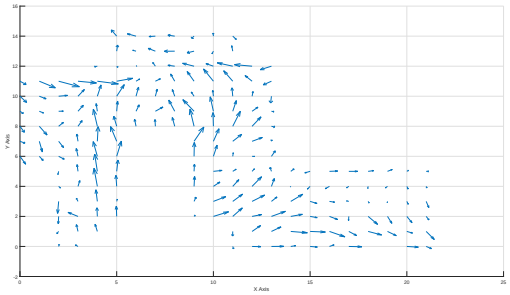

Figure 6.3: At Z=0.6 m

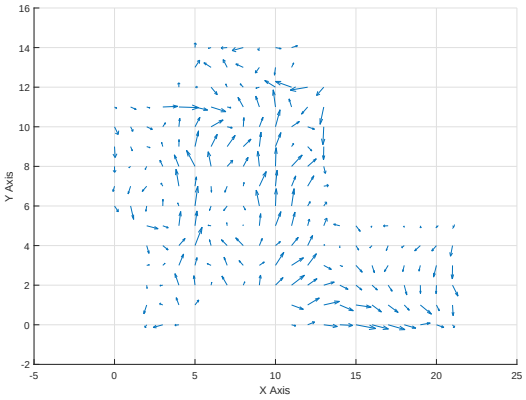

Figure 6.4: At Z=0.9 m

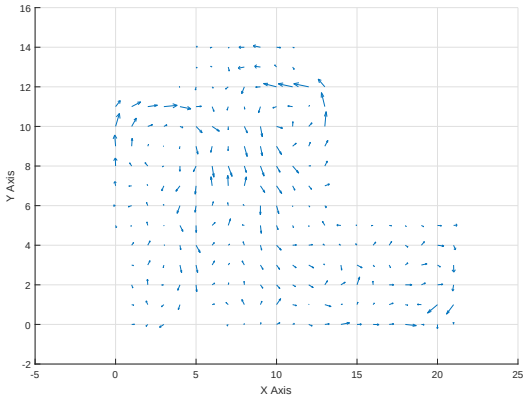

Figure 6.5: At Z=1.22 m

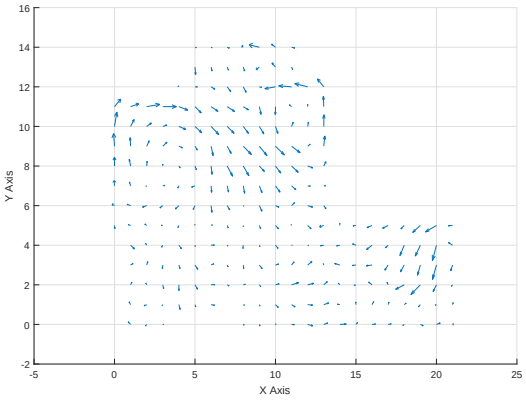

Figure 6.6: At Z=1.5 m

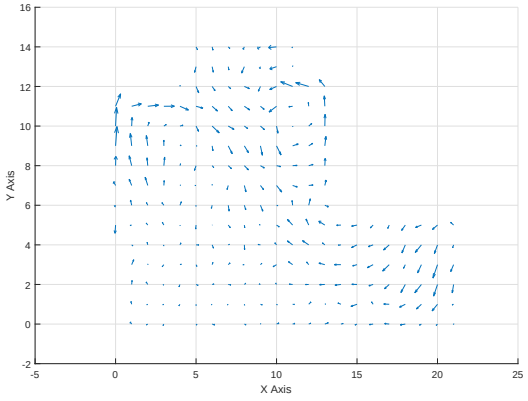

Figure 6.7: At Z=1.83 m

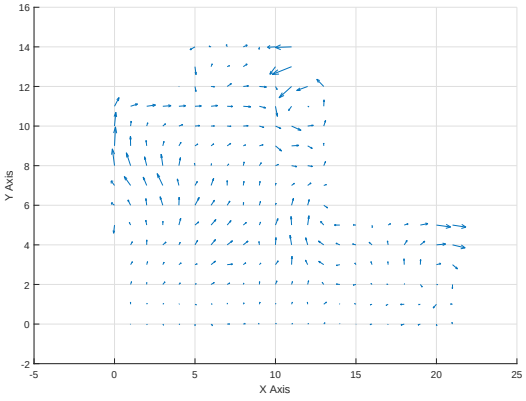

Figure 6.8: At Z=2.13 m

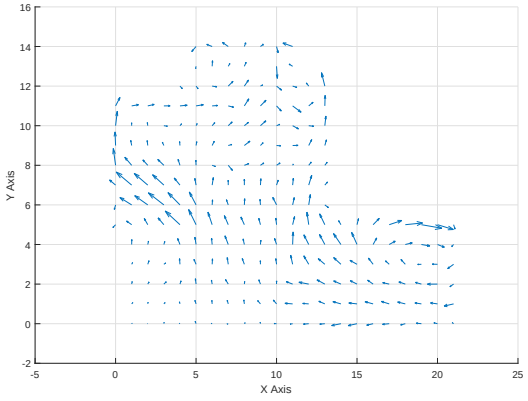

Figure 6.9: At Z=2.44 m

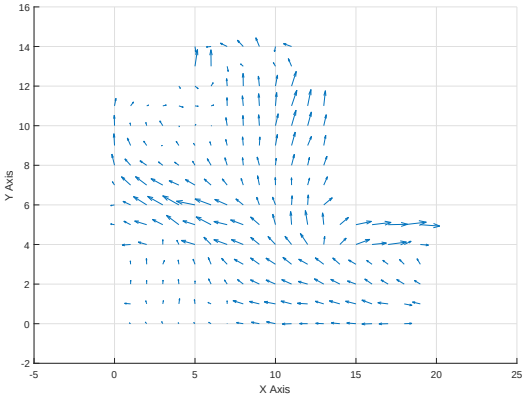

Figure 6.10: At Z=2.74 m

Appendix A.1. Two-dimensional resultants of air velocity in the XZ plane

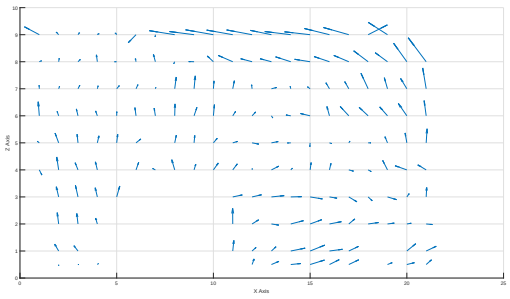

Figure 6.11: At Y=1

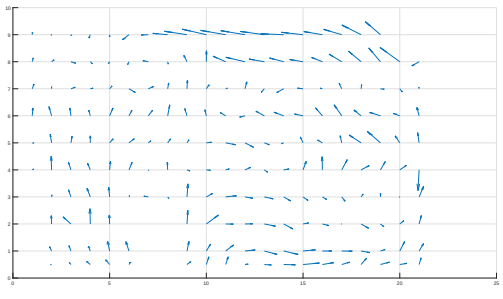

Figure 6.12: At Y=2

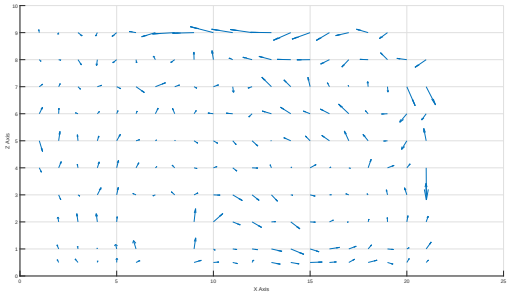

Figure 6.13: At Y=3

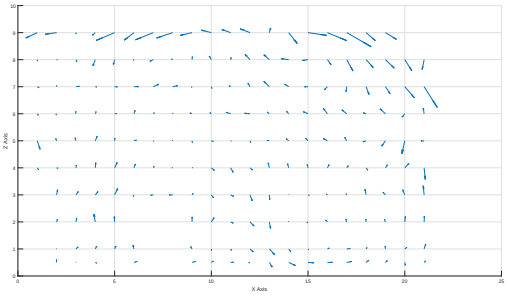

Figure 6.14: At Y=4

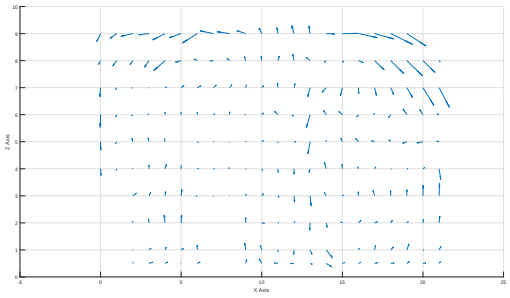

Figure 6.15: At Y=5

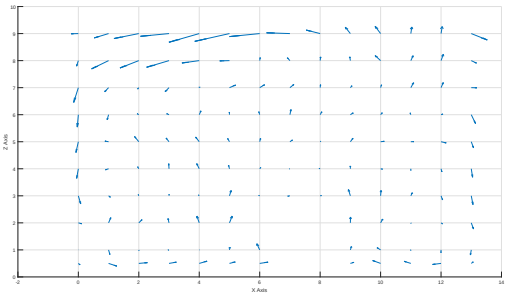

Figure 6.16: At Y=6

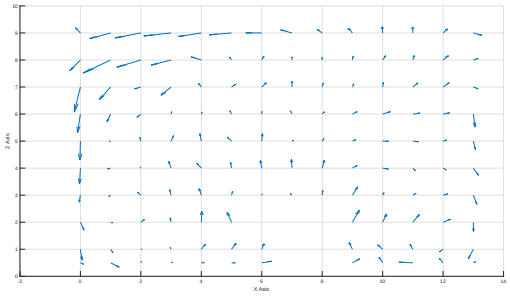

Figure 6.17: At Y=7

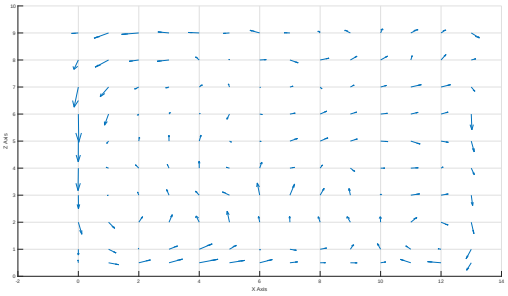

Figure 6.18: At Y=8

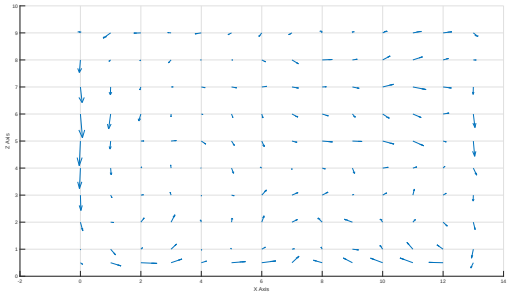

Figure 6.19: At Y=9

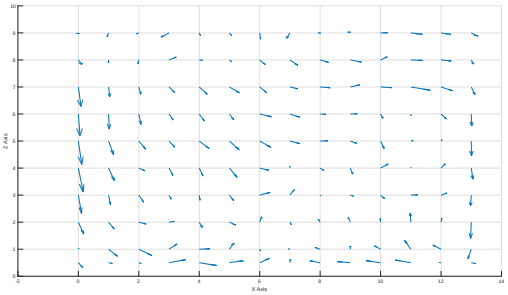

Figure 6.20: At Y=10

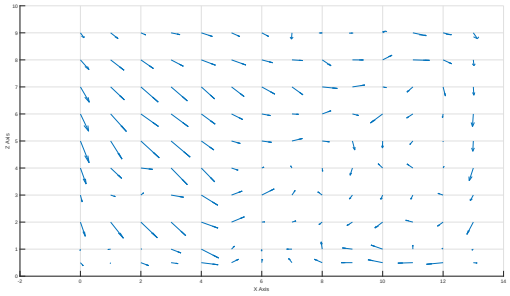

Figure 6.21: At Y=11

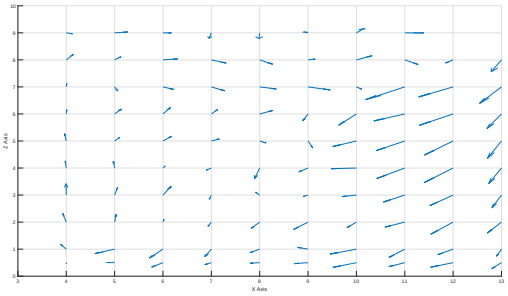

Figure 6.22: At Y=12

Appendix A.2. Two-dimensional resultants of air velocity in the YZ plane

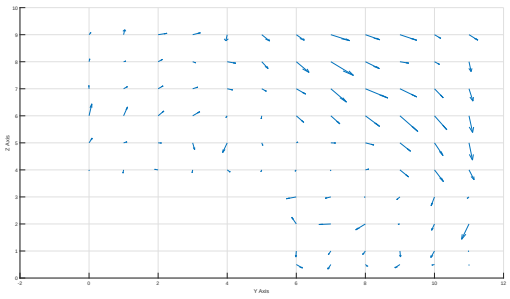

Figure 6.23: At X= 1

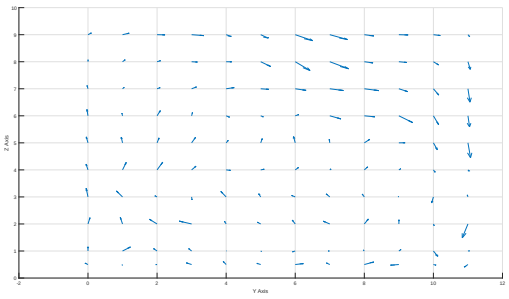

Figure 6.24: At X= 2

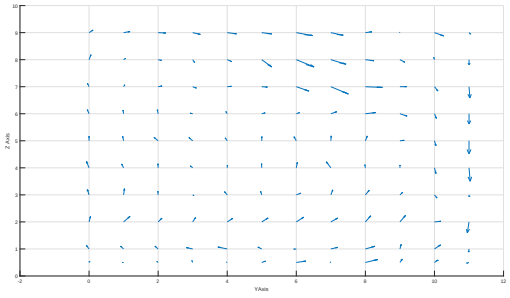

Figure 6.25: At X= 3

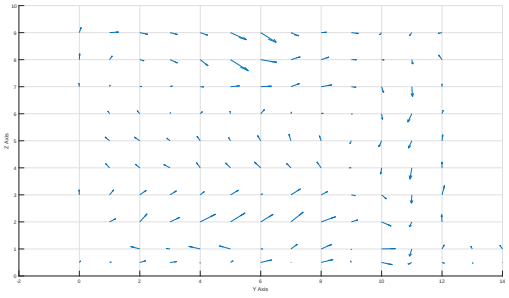

Figure 6.26: At X= 4

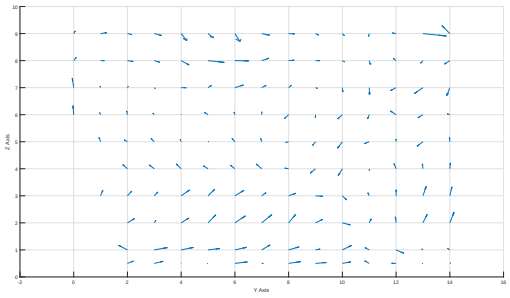

Figure 6.27: At X= 5

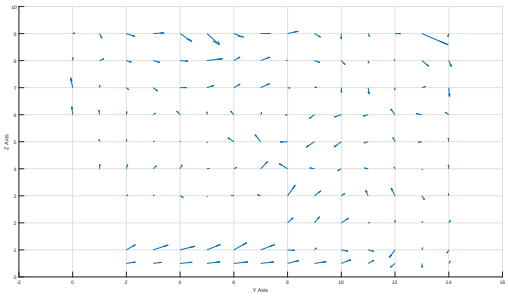

Figure 6.28: At X= 6

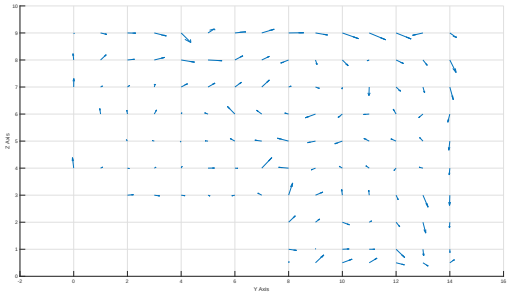

Figure 6.29: At X= 7

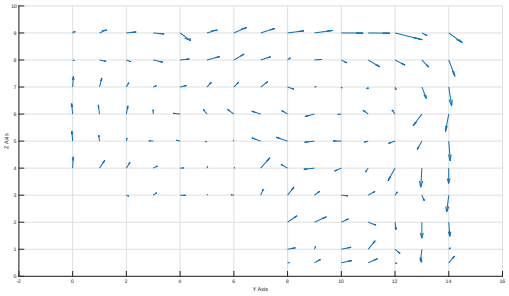

Figure 6.30: At X= 8

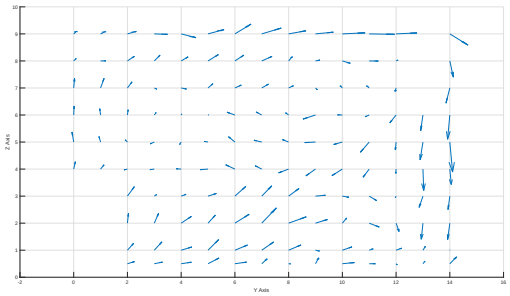

Figure 6.31: At X= 9

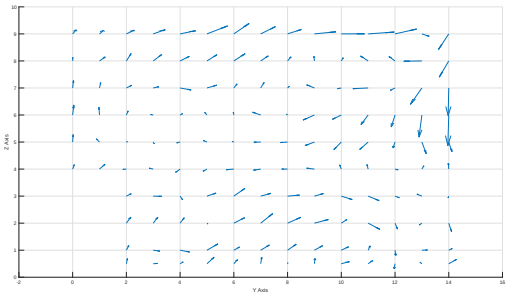

Figure 6.32: At X= 10

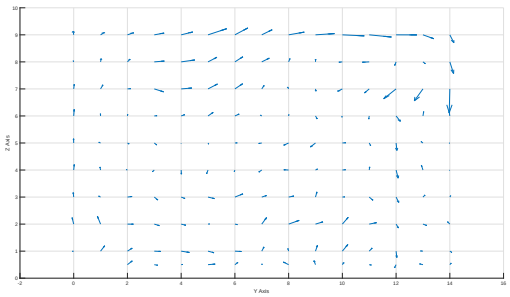

Figure 6.33: At X= 11

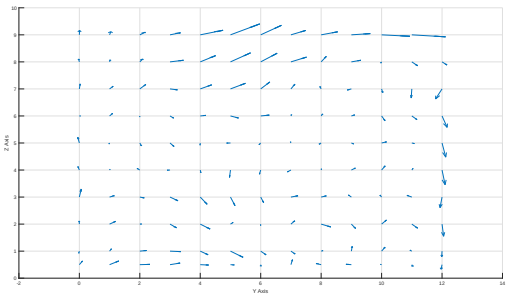

Figure 6.34: At X= 12

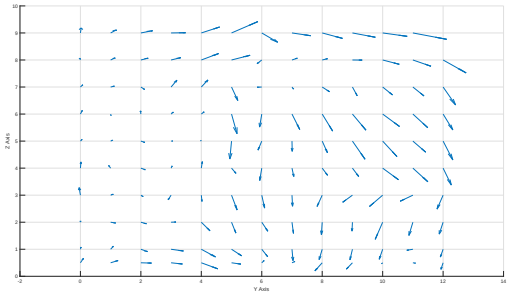

Figure 6.35: At X= 13

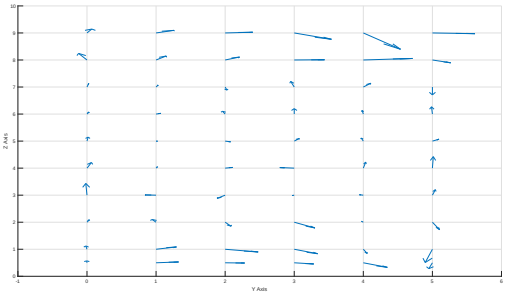

Figure 6.36: At X= 14

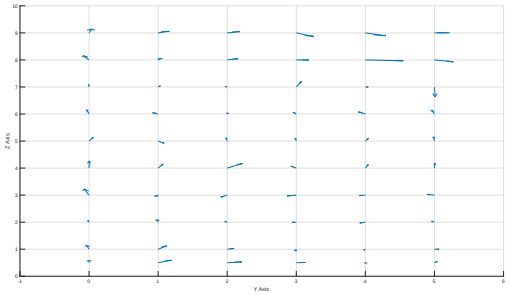

Figure 6.37: At X= 15

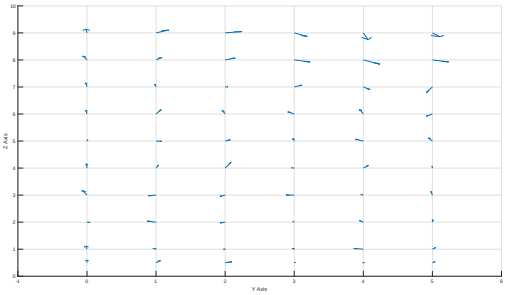

Figure 6.38: At X= 16

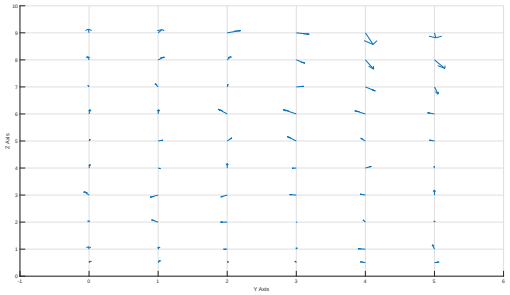

Figure 6.39: At X= 17

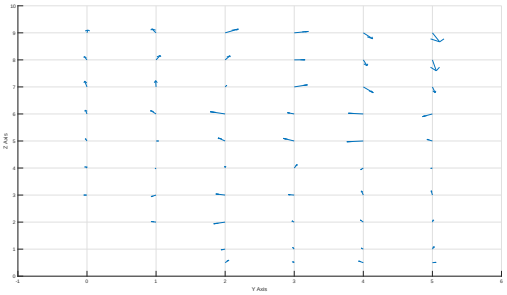

Figure 6.40: At X= 18

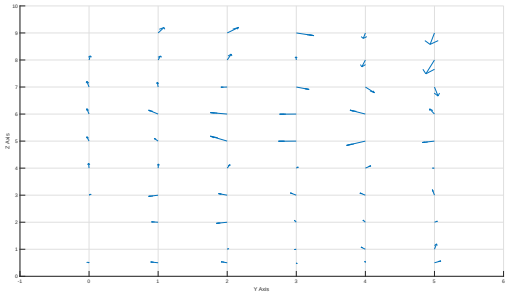

Figure 6.41: At X= 19

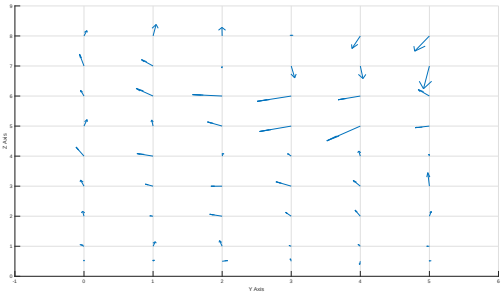

Figure 6.42: At X= 20